Micro & nanofabrication methods for nanoscience applications

Subtitle: toward 3D fabrication, manipulation and characterization

E. Di Fabrizio

LILIT (National Nanotechnology Laboratory), TASC-INFM Nanolithography beamline at ELETTRA Synchrotron Light Source, S.S.14 km 163.5, 34012 Basovizza, Trieste, Italy

email: difabrizio@tasc.infm.it

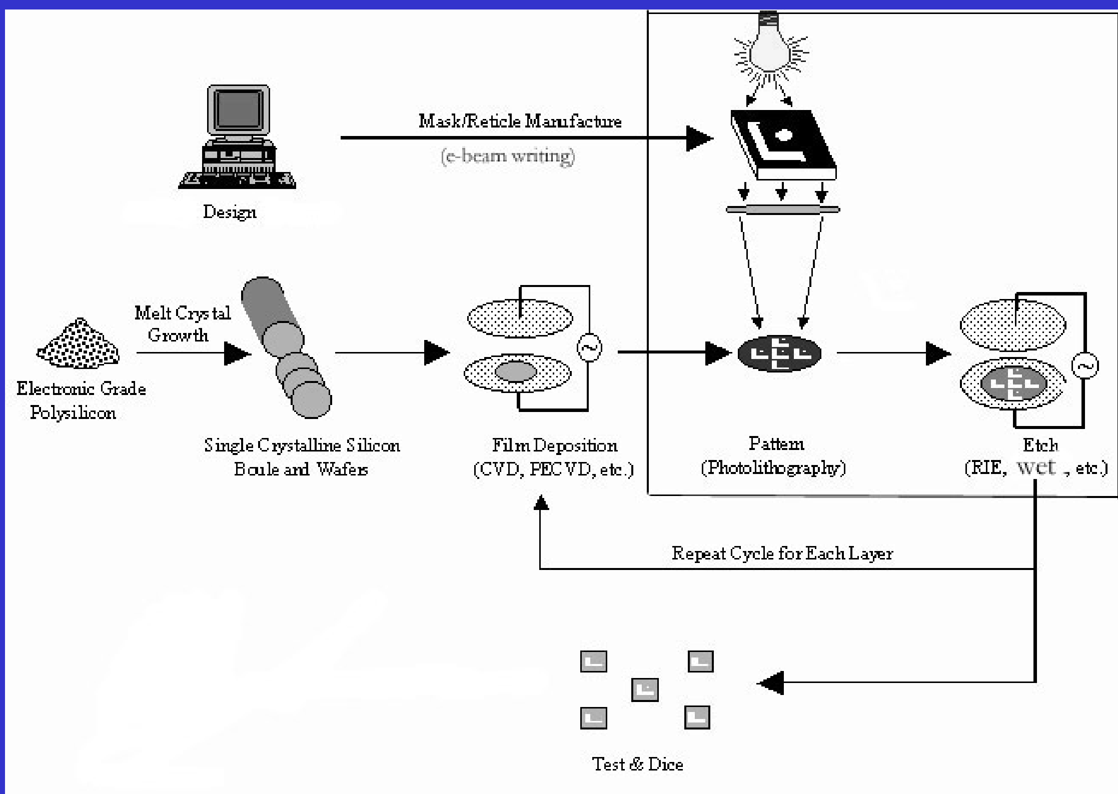

Scheme of a typical synchrotron X-ray lithography system

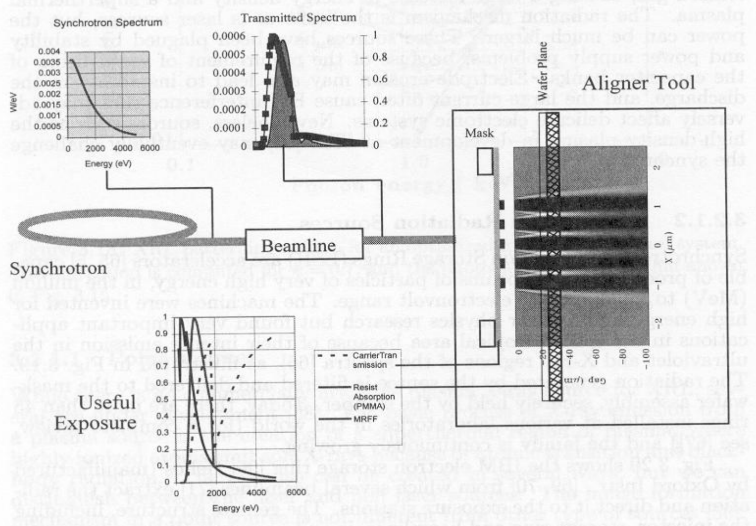

Figure 3.19: Schematic of an X-ray Lithography system based on a synchrotron. Notice the synchrotron, beamline and mask arrangement as well as the changes in the spectrum of the radiation.

XRL – masks 1X

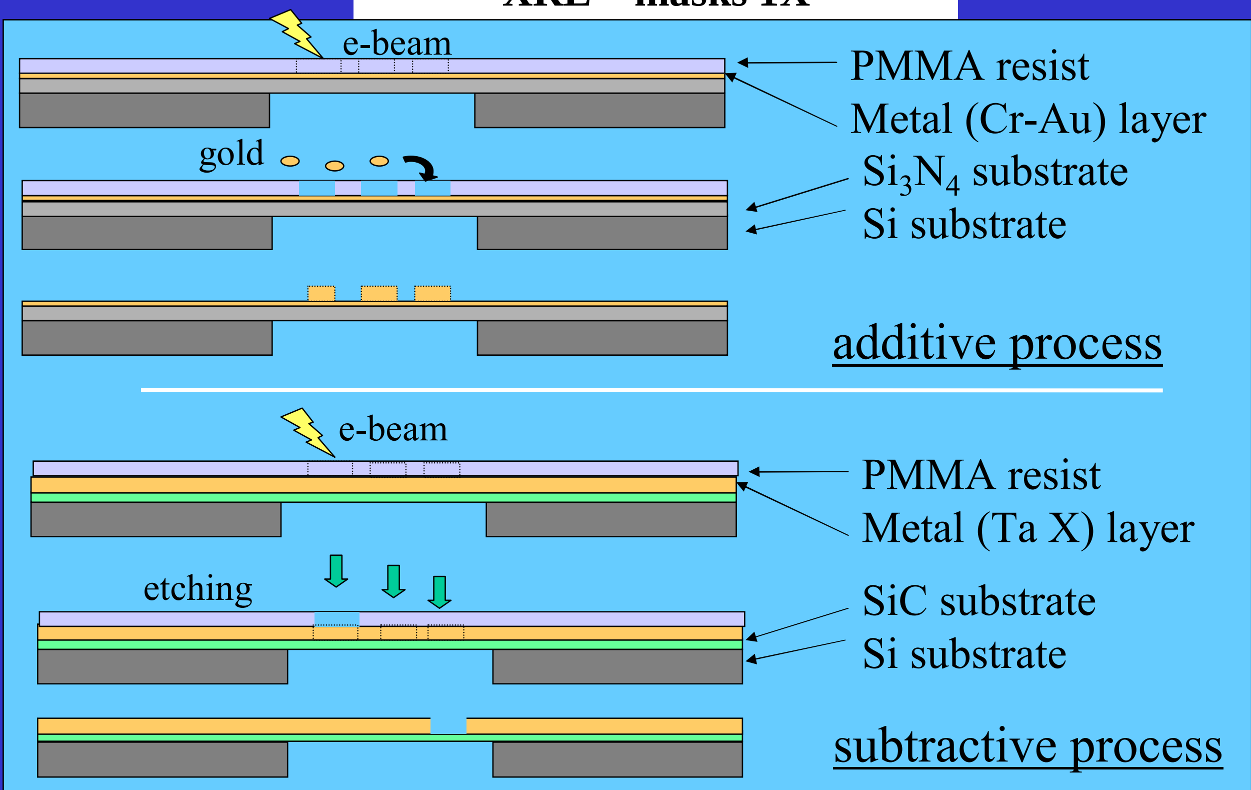

2D structured with X ray

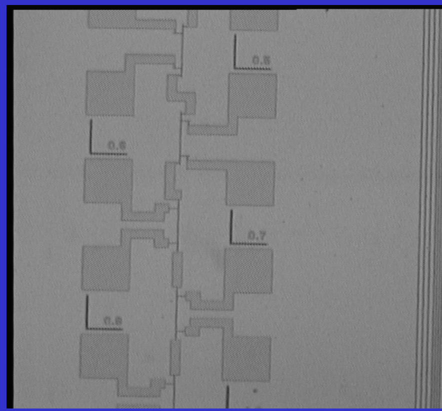

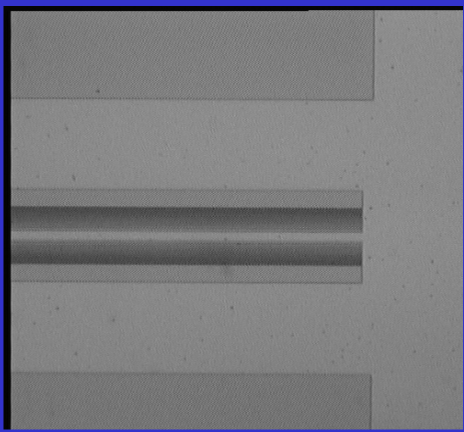

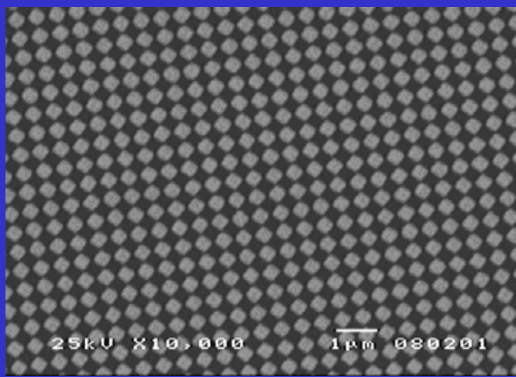

High resolution patterns

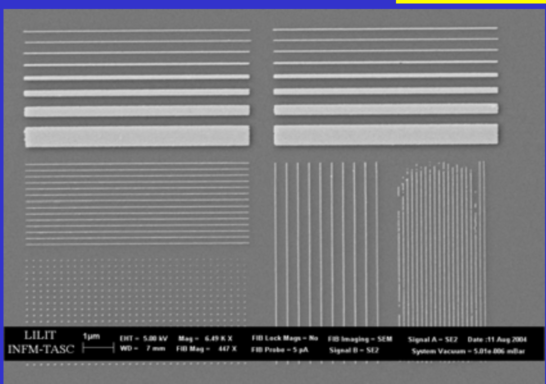

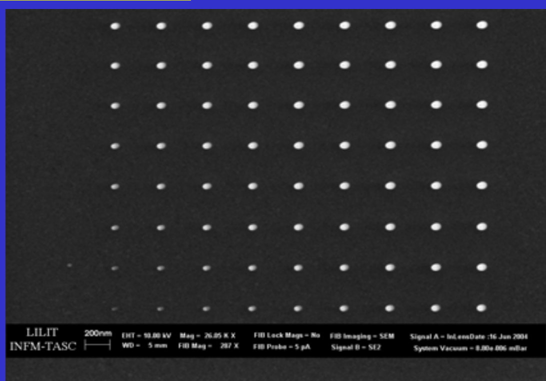

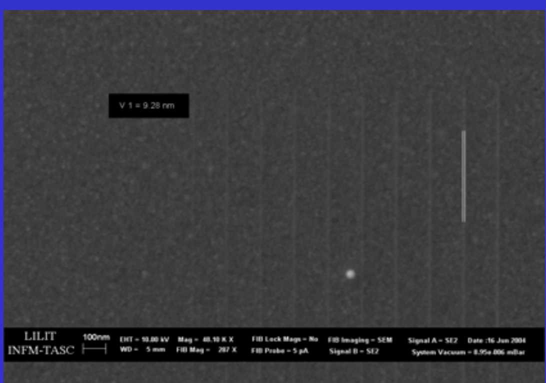

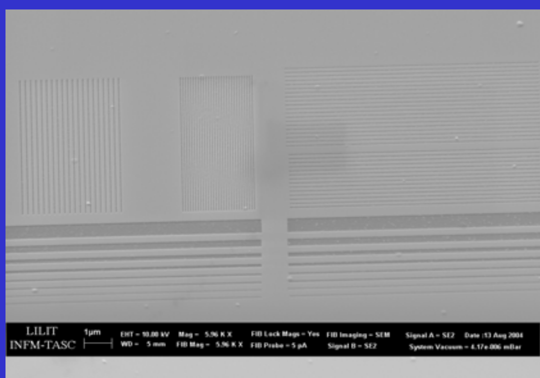

Objectives:

- Achievement of 3D resist microstructures in only one shot
- Modulation of the x-ray dose by using a grey tone mask

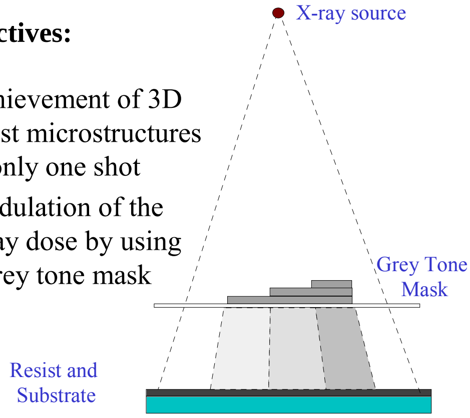

Simulation of illumination effect

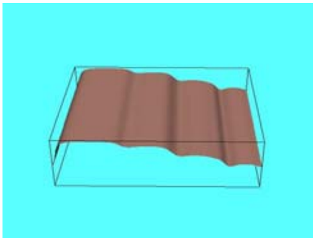

By computer simulation, we obtain this shape for the developed resist exposed by the x-rays passing through the described mask

Picture of the mask

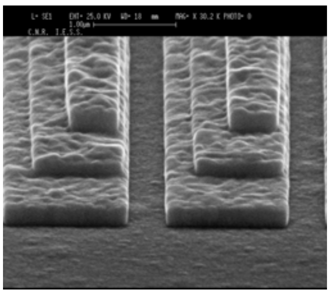

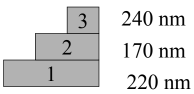

SEM image of 3D shaped resist

dose of 7000 mJ/cm2, and gap of 13 µm.

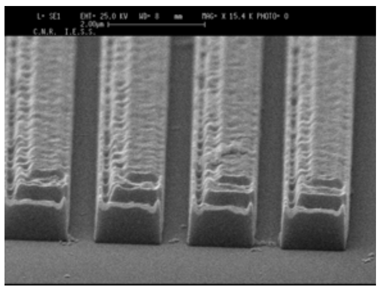

Multilevel Zone PlateFor hard X-rays (8-12 keV)

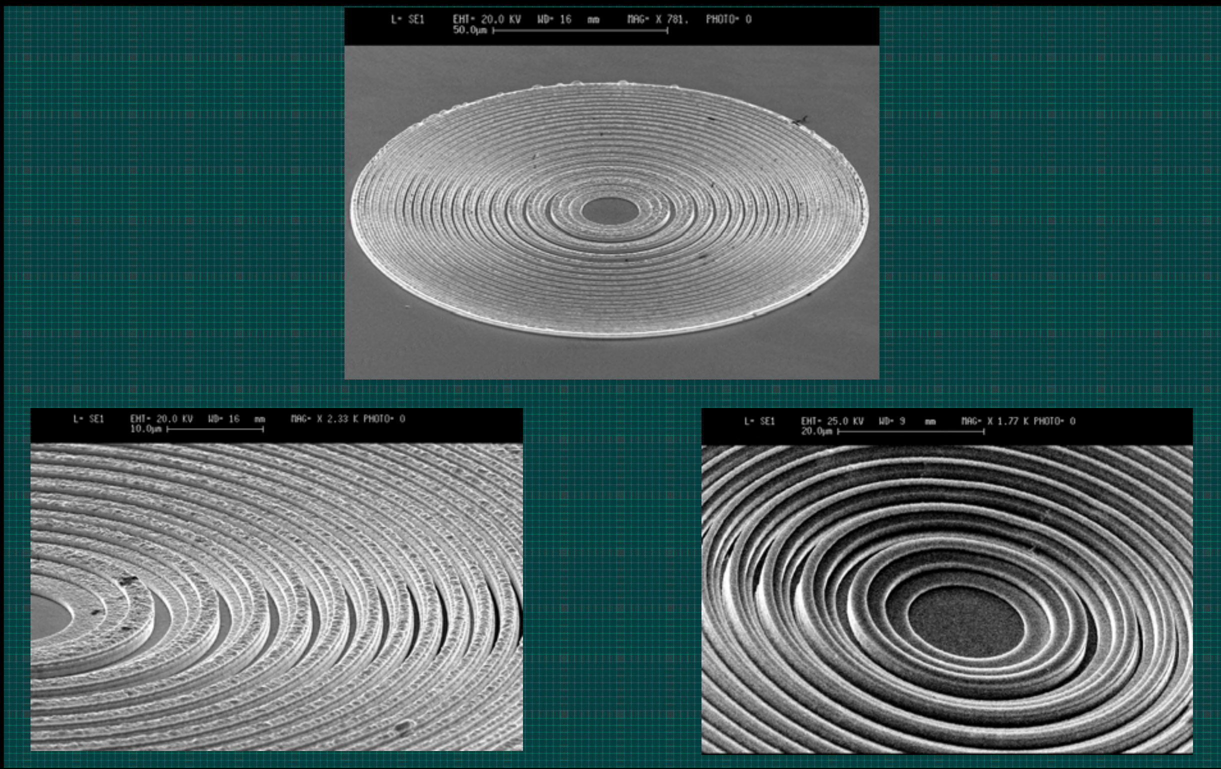

3D structuringflow chart

4µm PMMA
substrate

X-ray

X-ray

Metal electroplating

Resist stripping

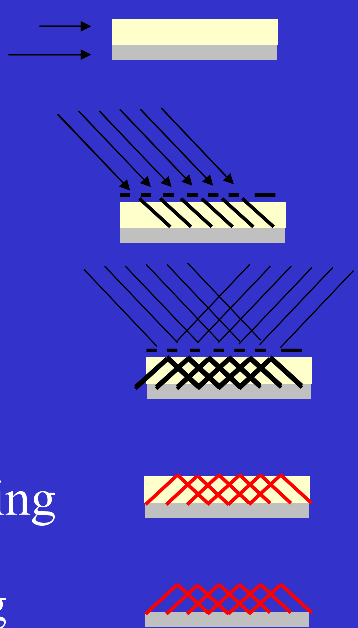

Tilted stage for 3D exposures

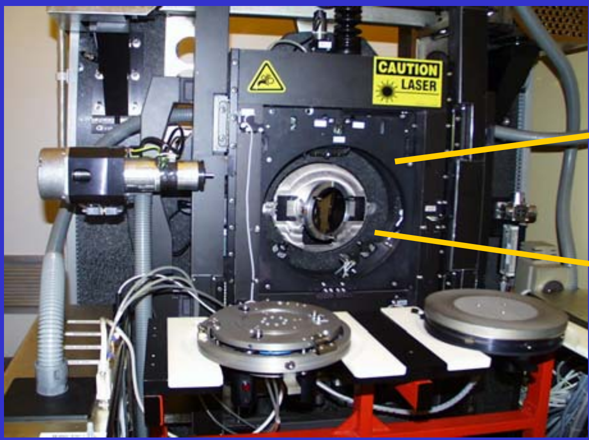

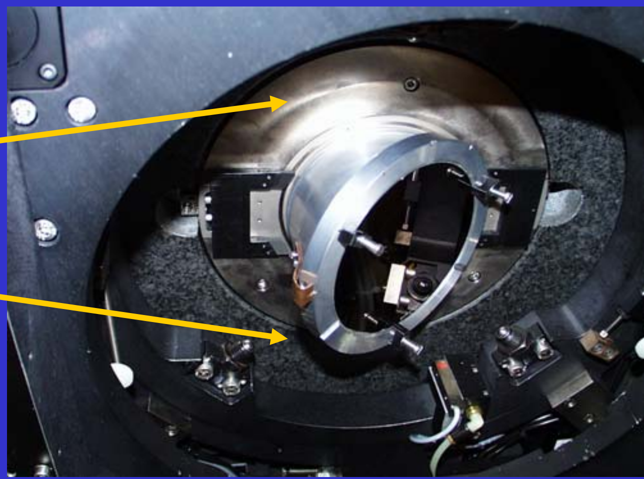

Tridimensional structures

3D PH. Crys. By X-ray litho

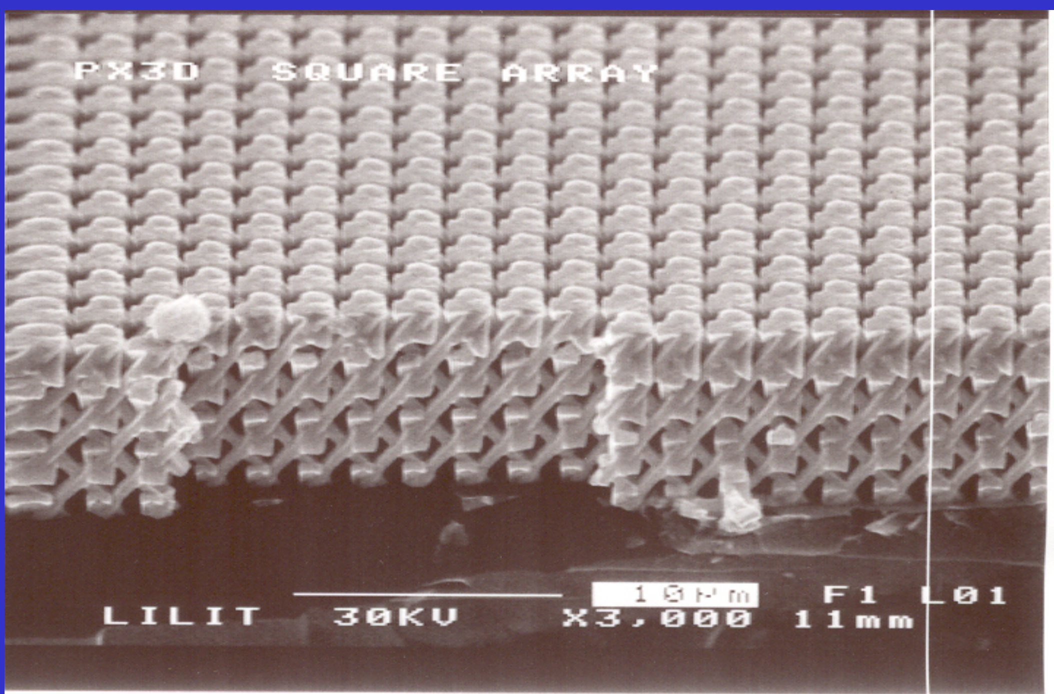

Combination of EBL and X-ray lithography (see Poster #BM-P03 F. Romanato et al. Patent pending June 2003)

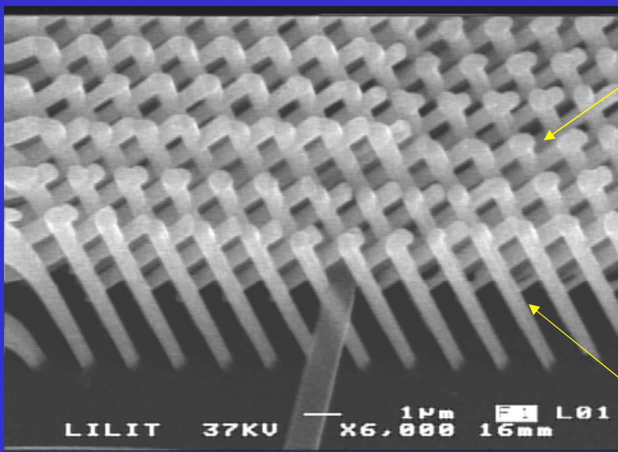

High speed fabrication needs parallel processes

X-ray

Defect generation needs serial litho

EBL

3D building block for microfluidic

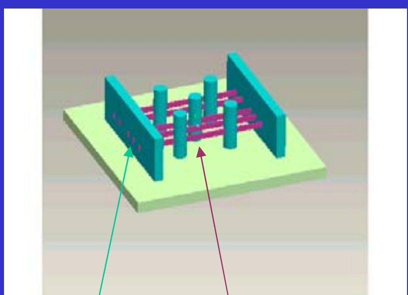

Neg. resist

Posit. resist

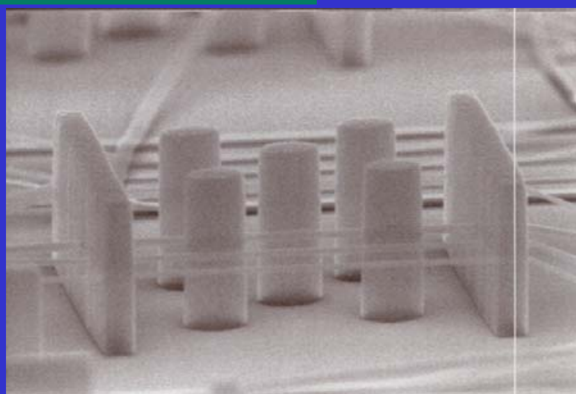

After electroplating growth →

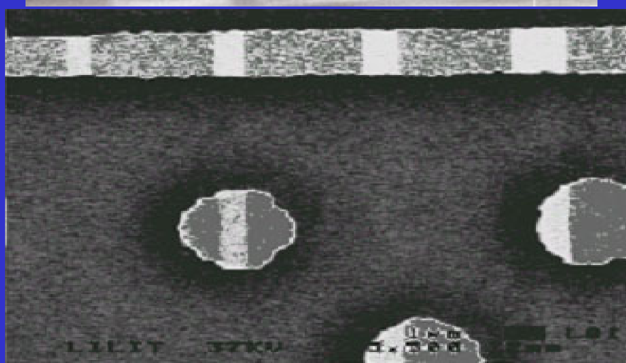

NanoImprinting

Stamp materials : Si, Si oxide, Si nitrate,Ni, W, quartz, sapphire

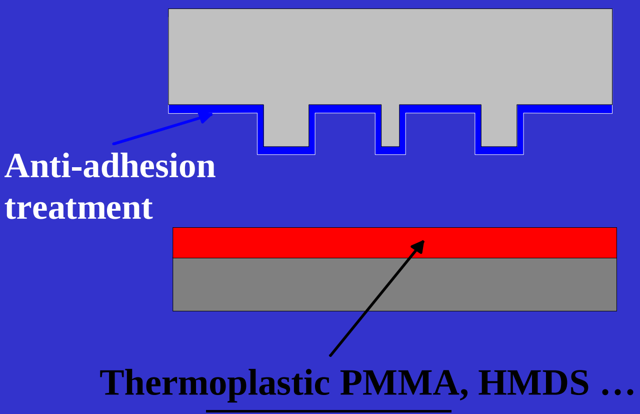

Embossing conditions

pressure: 50-100 bar

temperature: T ~ T_g+ 90°

Patterning by Nanoimprint

Master: Gold on Silicon

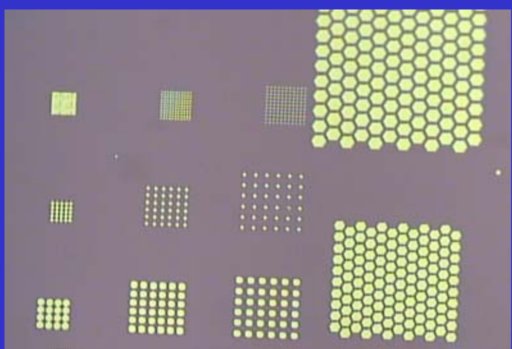

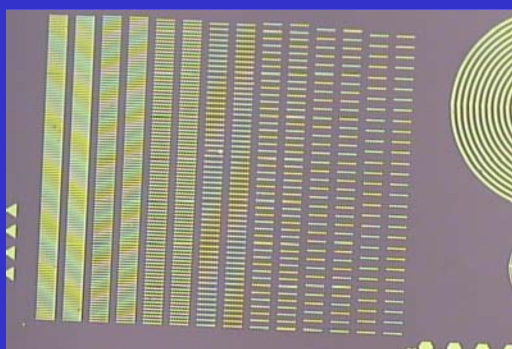

Imprinted structures: PMMA (plexiglass) on Silicon

High resolution Imprinting lithography

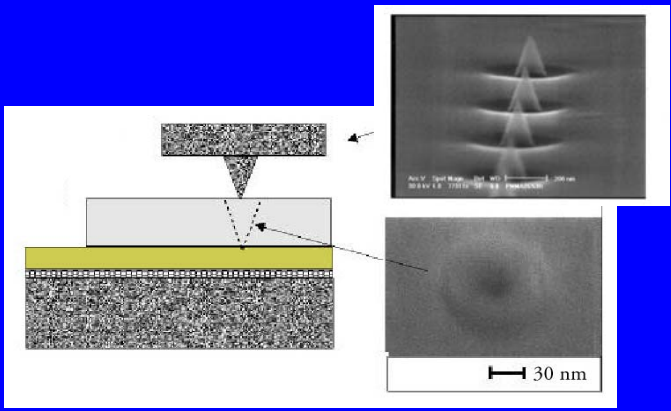

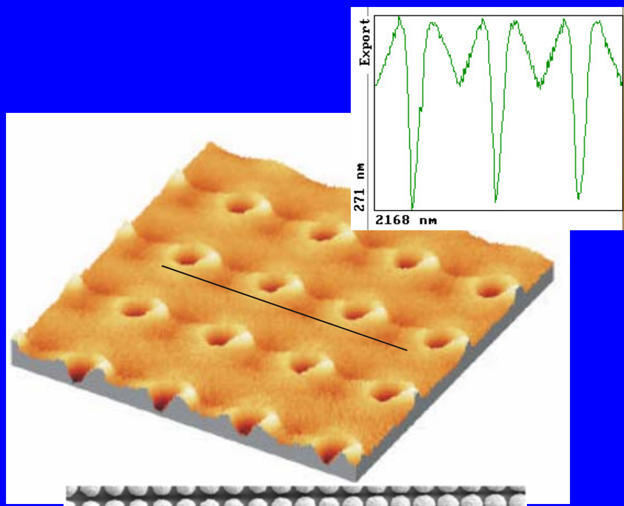

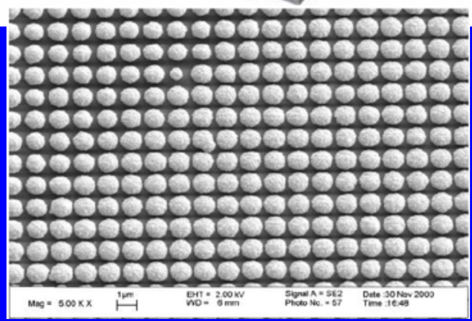

Resolution: 6 nm (limited by master)

Placement accuracy: 30 nm for a field of 30x30mm²

Alignment: 0.5µm over 4" wafers

Throughput: ~20 w/h

3D patterning by Nanoimprint

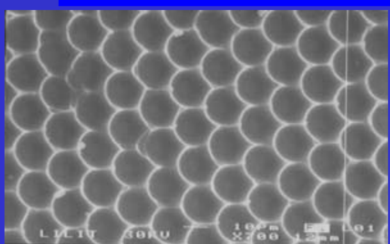

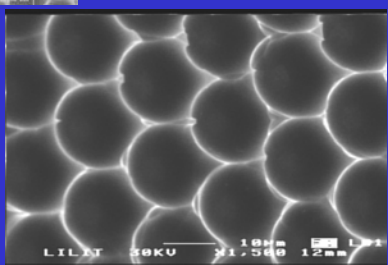

Glass Master

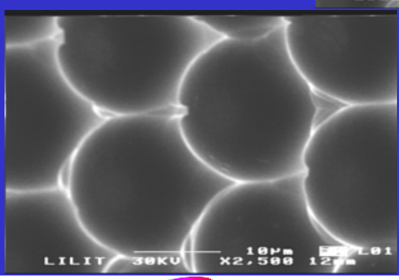

Lenses imprinted in thermoplastics

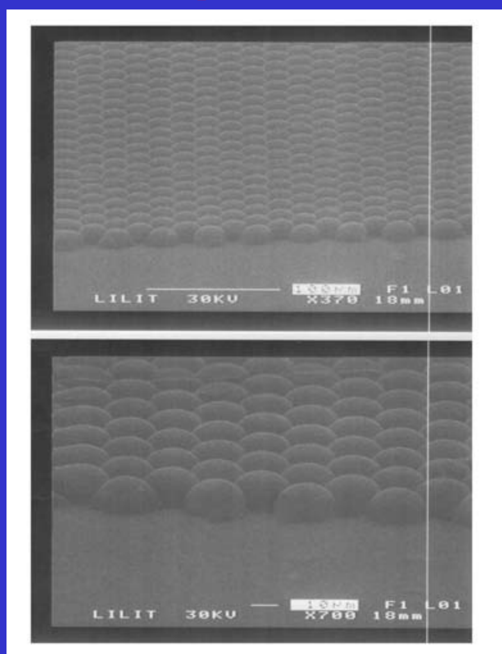

Toward 3D structures:combination of : Imprinting & X-ray litho

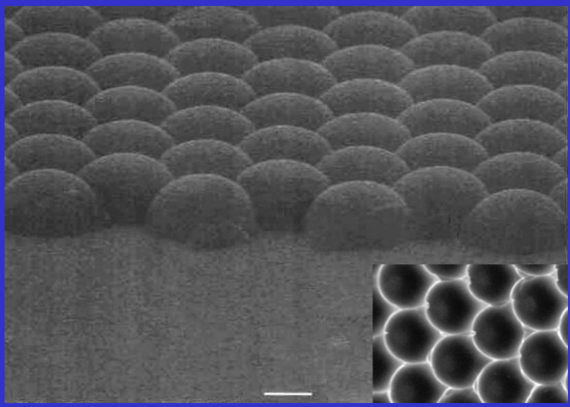

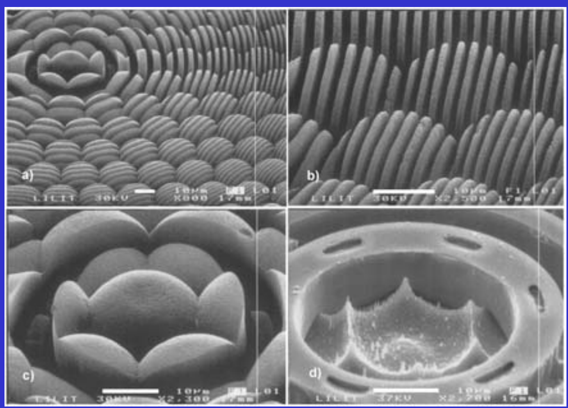

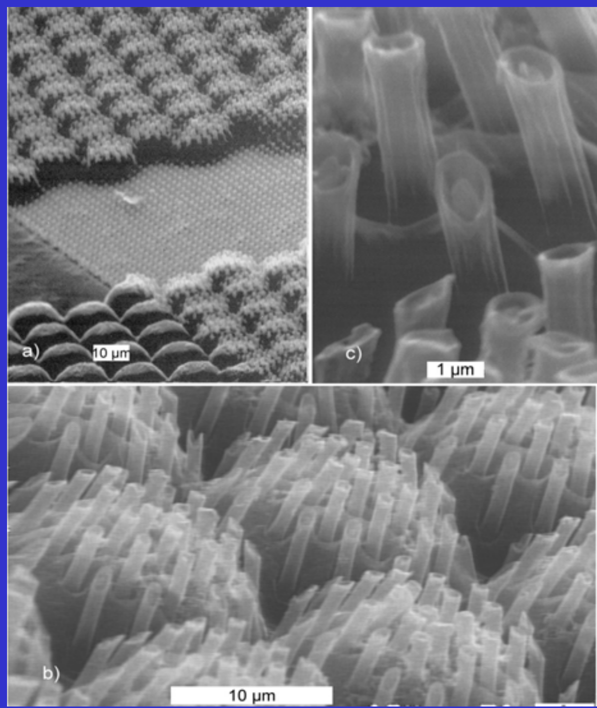

Two Photon Absorbtion (TPA) induced Microfabrication

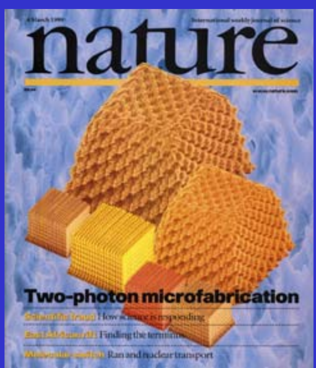

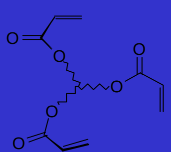

2hν

D-π-D TPA dye

Insoluble cross-linked polymer

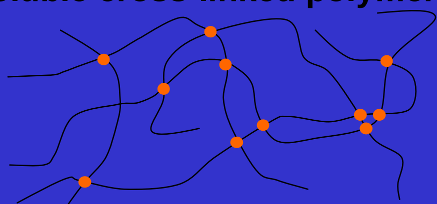

100 fs pulses 700 - 800 nm

1.4 NA , 0.35 µm spot size

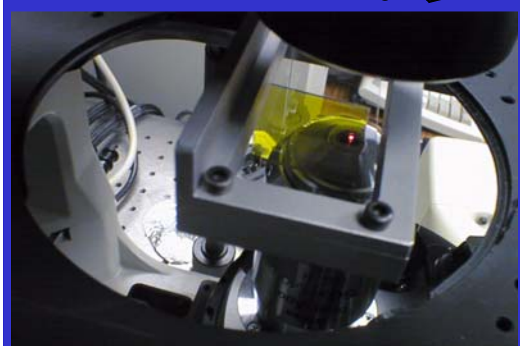

Maruo, Nakamura, Kawata, *Opt.Lett.* 1997
Wu, Webb *et al.*, *Proc. SPIE* 1992

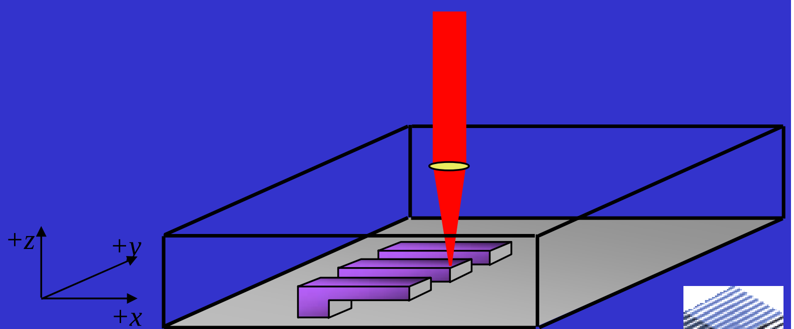

Two photon lthography

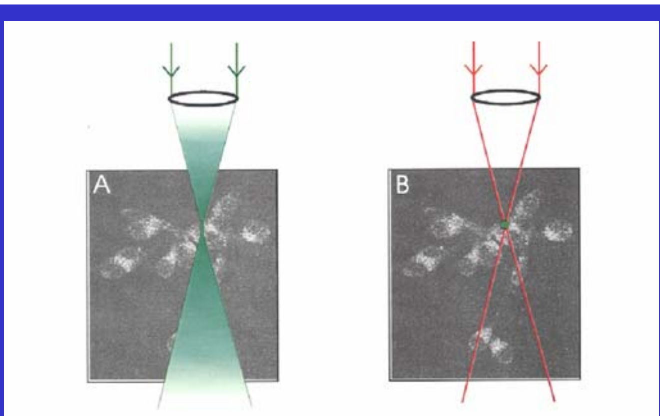

FIGURE 13-1 Illustration of excitation-light path in wide-field epifluorescence or confocal (*A*) microscopy and two-photon excitation microscopy (*B*). In (*A*), the illumination occurs throughout the field of view, whereas in two-photon-excitation fluorescence microscopy, it is limited to a spot at the focal plane of the infrared laser beam.

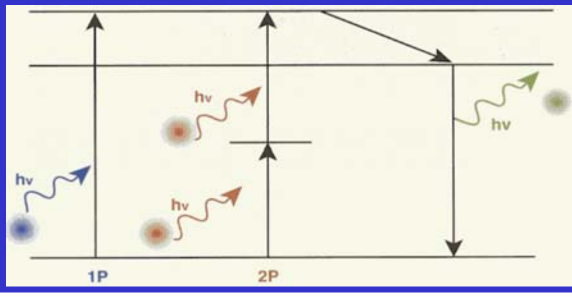

FIGURE 3-8 Spatial extension of the fluorescence emission from a solution containing fluorescent molecules under one- and two-photon excitation. In the case of TEP, the excitation phenomenon, small spots in the lower part of the cuvette, takes place only within a diffraction-limited volume. This volume can be roughly quantified using the resolution parameters of the system. In the case of conventional or one-photon excitation, the double-cone geometry (the upper bright area in the cuvette) is evident. The main implications of this behavior are an inherent confocal effect and consequent optical sectioning property, and photobleaching and phototoxicity confined to a sub-femtoliter volume. (Picture courtesy of John Girkin from Biorad web homepage.)

2Photon absorbtion $\propto I^2 \propto \dfrac{1}{r^4}$

Two-Photon Lithography

$2\,h\nu = \Delta E$

2-photon probability ~ (light intensity)^2

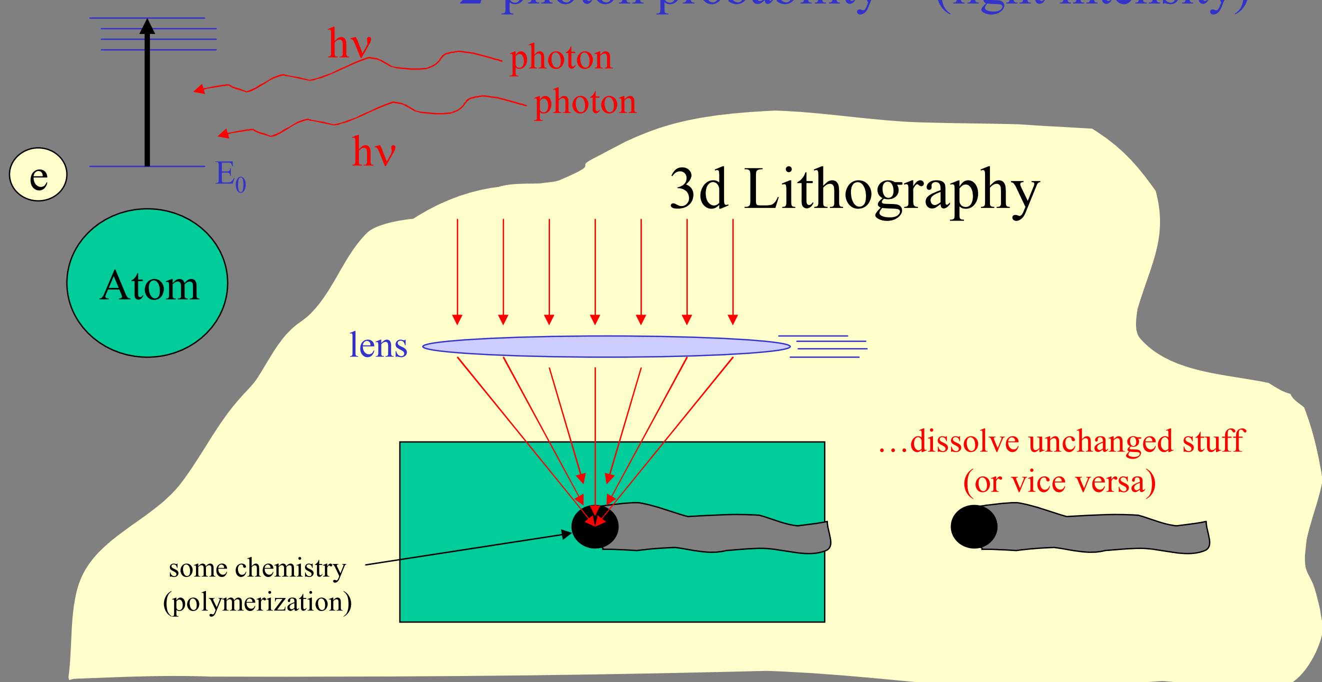

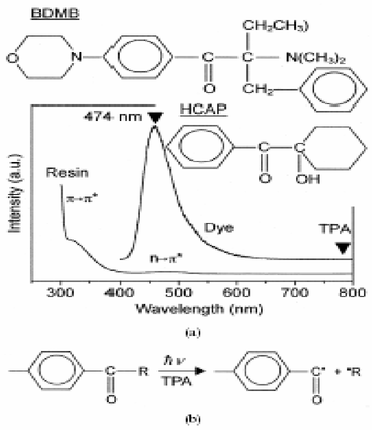

Fig. 2. (a) The absorption spectrum of resin, a mixture of urethane acrylate monomer/oligomer and two kinds of benzoyl initiators, for short, BDMM and HCPA (the inset). The emission spectrum of a fluorescence dye used for 3-D microdiagnosis (see Section VIII) is also shown. (b) Typical reaction of radical production via an α-cleavage process. Radicals are produced in HCAP entirely by and in BDMB mostly by this mechanism. Note negligible single photon absorption at the working wavelength of 780 nm.

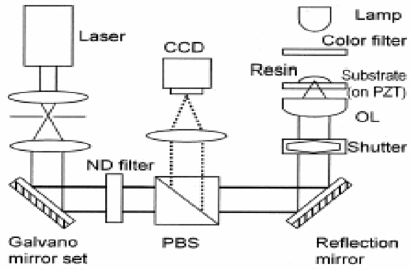

Fig. 3. Schematic two-photon laser precision microfabrication system. The use of femtosecond laser and tightly focusing light by a high NA lens (1.4, oil immersion used here) is critical to launch the TPA polymerization process. The output stability of laser pulse energy and the accuracy of focal spot/sample scanning are the most important factors that guarantee a high precision fabrication. The imaging system using an CCD camera is useful both for optical adjustment and for *in situ* fabrication monitoring. PBS: polarization beam splitter; OL: objective lens.

actual reactions involved in practical photopolymerization systems were more complicated, however, the principle of electron excitation, radical generation, and chain photopolymerization is as described above.

III. Laser Precision Microfabrication System

Typical cross sections for one- and two-photon processes are

Mode locked Ti:sapphire laser

- wavelength: 790 nm
- pulse width: 120 fs
- repetition rate: 76MHz
- peak power: 50mW

S. Maruo et al., Optics Lett. 22, 132 (1997)

Lithography: ealry attempts for 3 D

Let's make a "fusillo"

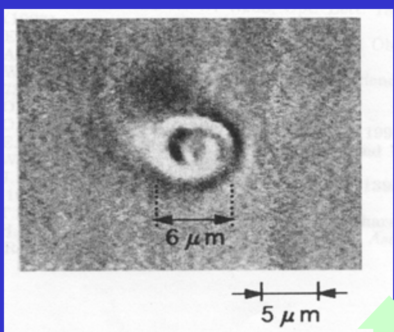

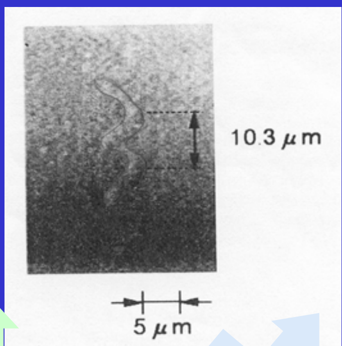

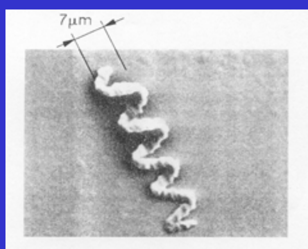

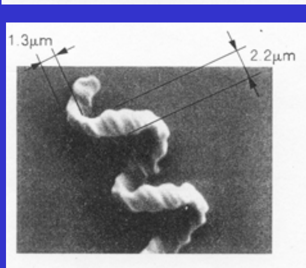

- imput power: 20mW 34mW
- time exposure: 2.3 s 1.4 s

S. Maruo et al., Optics Lett. 22, 132 (1997)

Collaboration with S. Kawata (Japan)

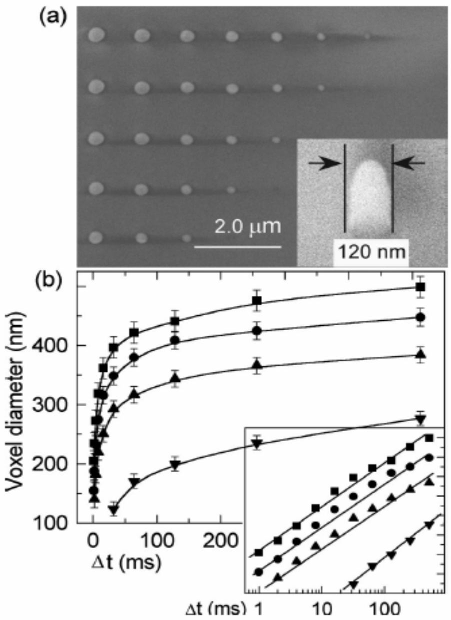

FIG. 2. Experimental evidence of SDL spatial resolution. (a) A SEM image of voxels obtained in different TPA exposure conditions. (b) Exposure time, Δt-dependent spatial resolution. The inset presents the same data but using a half-logarithmic coordinate. For different curves, the laser pulse energies (from top) are 163, 137, 111 and 70 pJ, respectively.

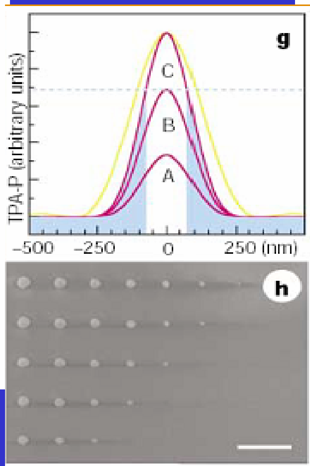

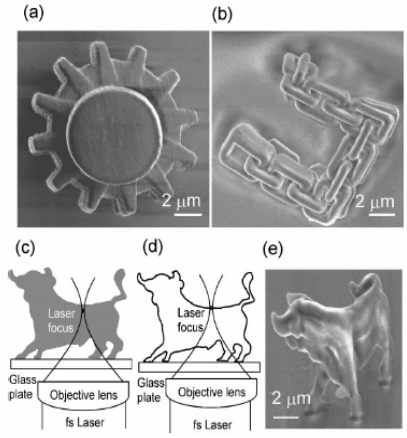

FIG. 3. Application examples of the SDL technique. (a) A micro-gearwheel, (b) a micro-chain, and (e) a micro-bull. (c) and (d) illustrate two different scanning modes: raster scanning and profile scanning.

Lithography is a Beast

[S. Kawata *et al.*, *Nature* **412**, 697 (2001)]

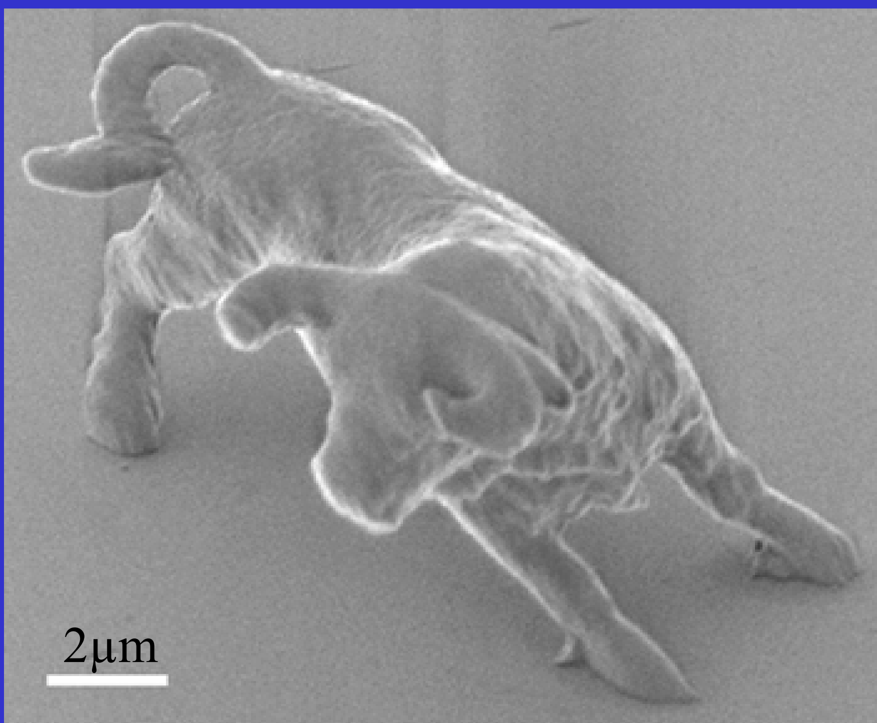

λ = 780nm

resolution = 150nm

7μm

(3 hours to make)

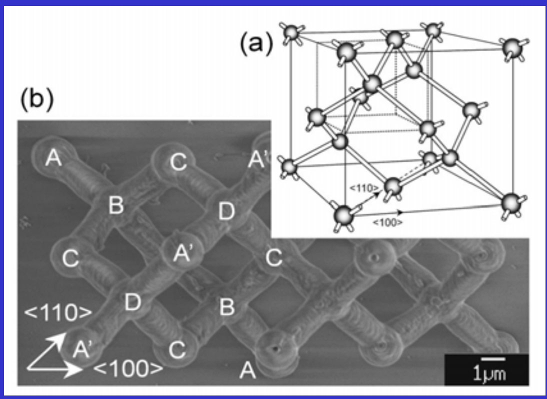

3D photonic crystal: "direct writing"

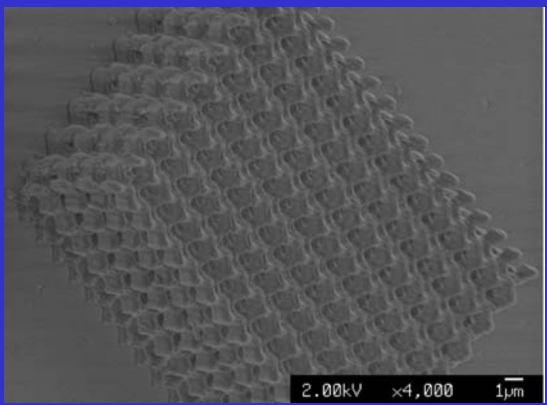

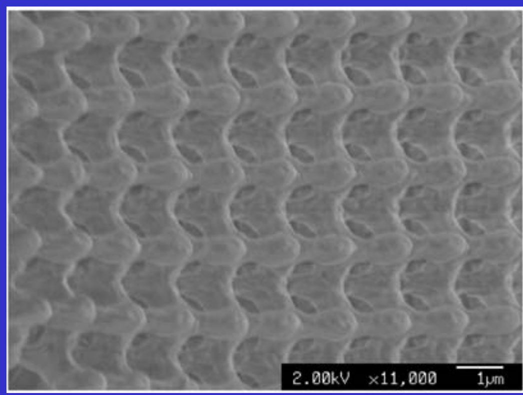

metal deposition with TPA: Silver Nanoparticles deposition

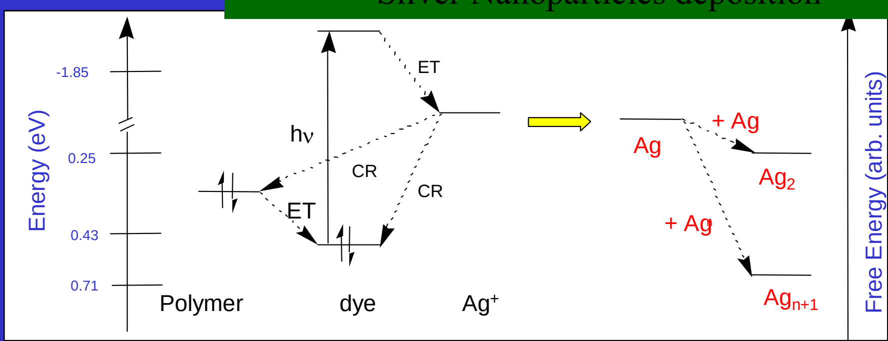

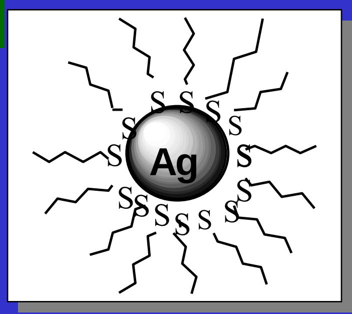

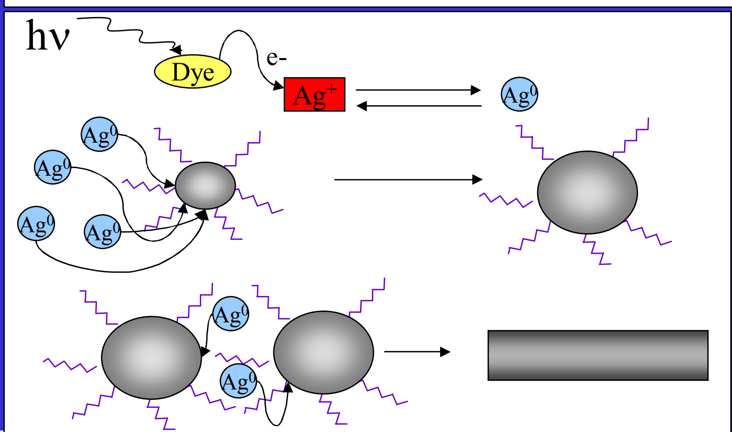

1. Photo-reduction

2. Growth

3. Coalescence

F. Stellacci, Adv. Mater. 2002, 14, No. 3, February 5

3D Metal Structures

Schematic Drawing

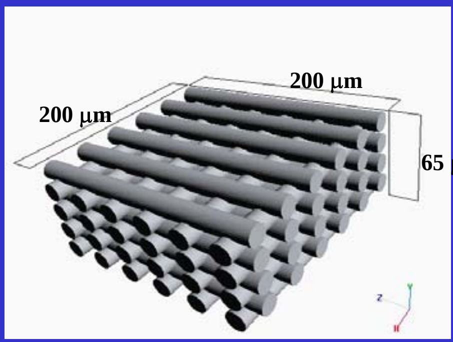

Wavelength: 730 nm
Pulse duration: 120 fs
Average Power: 15 mW
Writing Speed: 25 µm/s

Two-Photon Microscopy

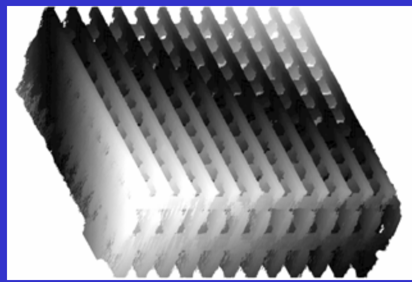

Scanning Electron Microscopy

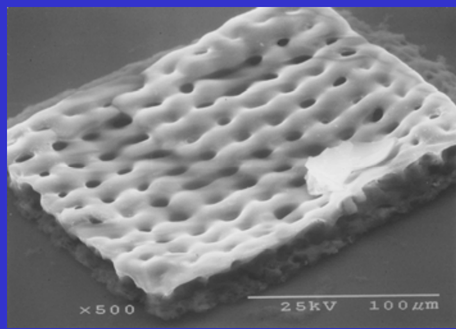

Transmission Optical Microscopy

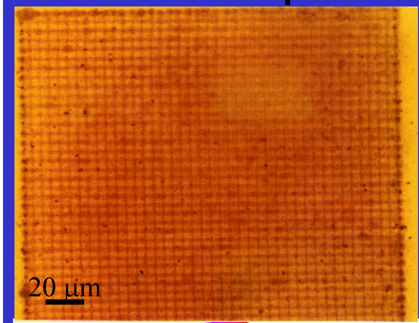

LEO 1540XB CrossBeam® Workstation

System Features:

- Super Eucentric 6-axis stage X 102 mm, Y 102 mm
- Gas injection system
- 4" Airlock (optional)
- Automated aperture change on FIB column
- Enhanced vacuum system

Options:

- EDS
- CAD
- Lithography
- SIMS

Beam deposition and gas assisted etch

LEO

Deposition

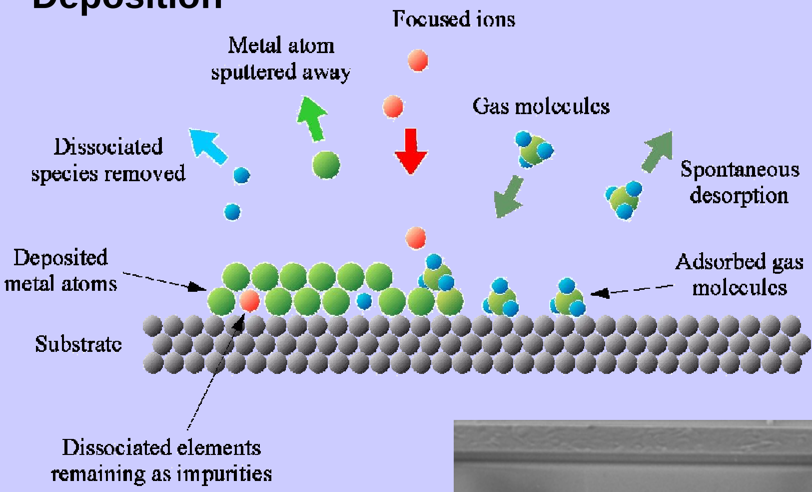

1. Adsorption of the precursor molecules on the substrate
2. Ion beam / e-beam induced dissociation of the gas molecules
3. Deposition of the material atoms and removal of the organic ligands

Available on LEO CrossBeams:

Metals:	W, Pt
Insulator:	SiO_2

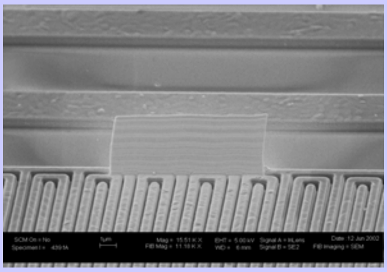

Tungsten wall

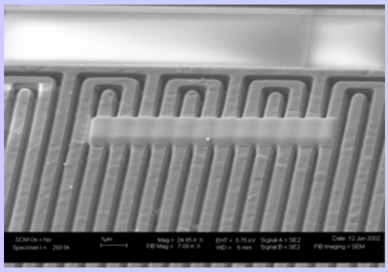

Tungsten deposition

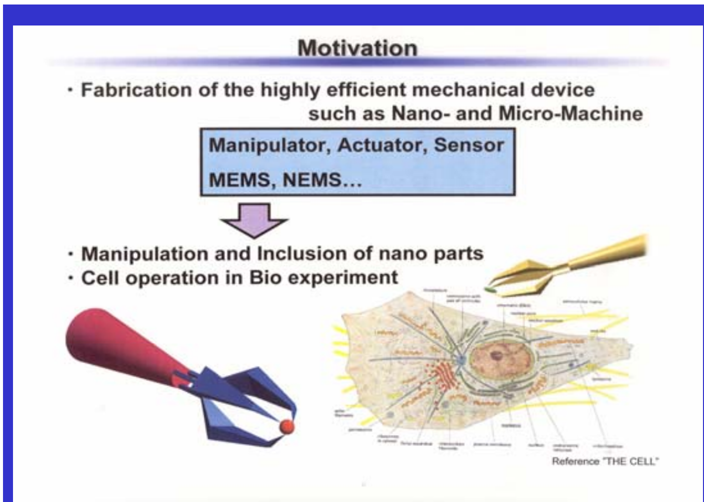

3D fabrication by FIB (S. Matsui Kyoto Univ)

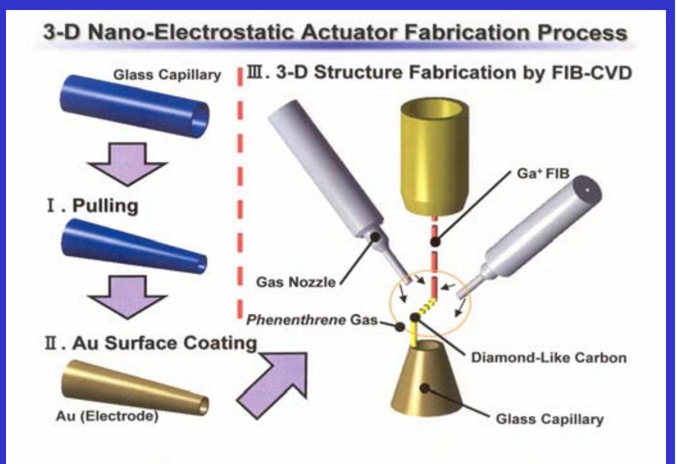

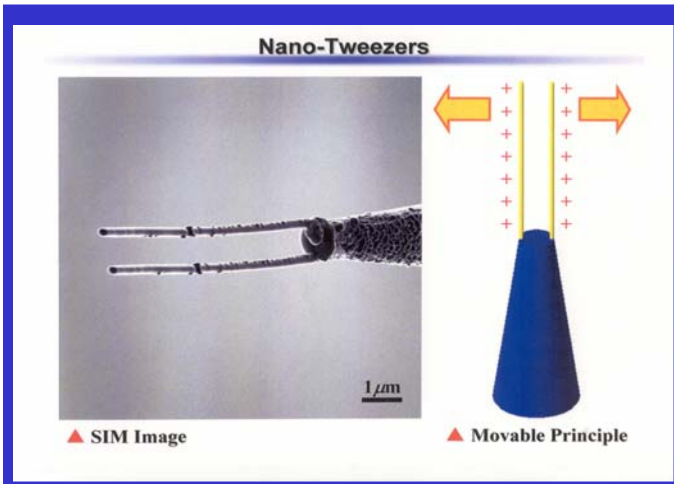

3D mechanical nanomanipulators

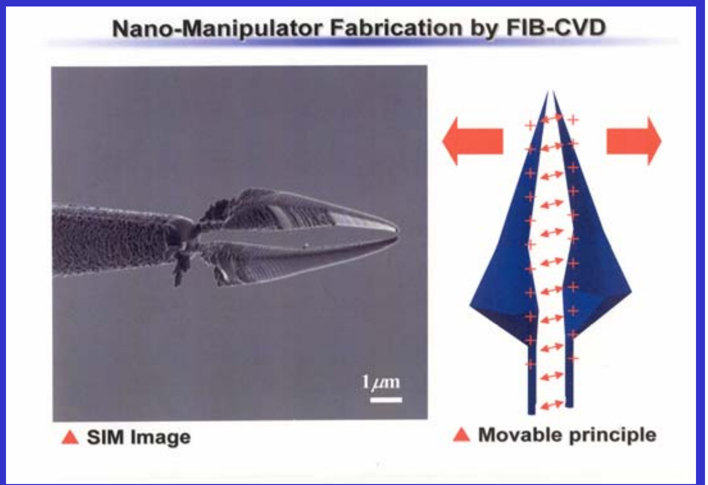

FIB on AFM tip

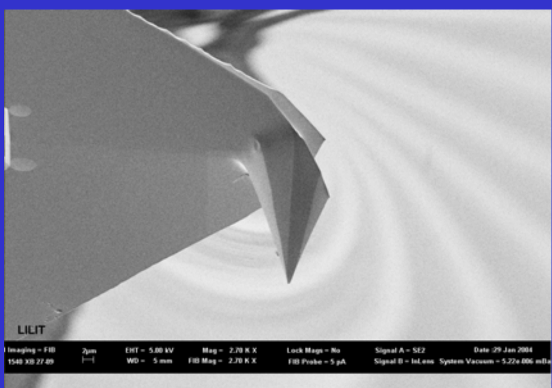

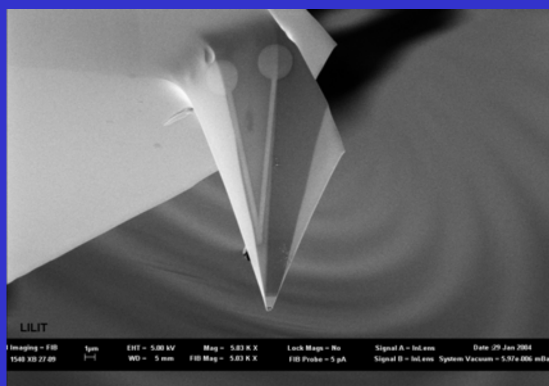

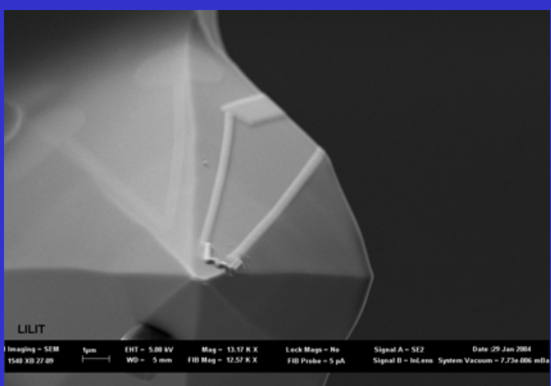

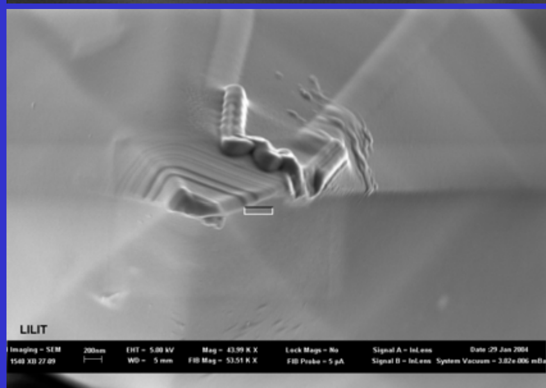

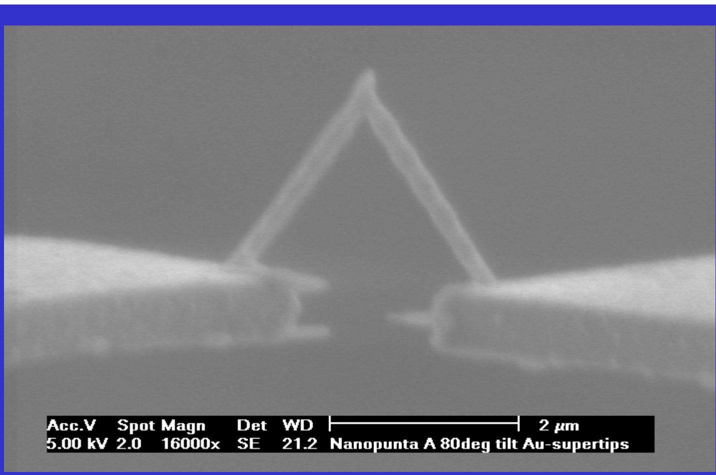

Ion/ electron deposition
Gold super tip on
Selfstanding Ni Tip
(Collboration Ivo Utke, Patrick Hoffmann
EPFL Lausanne)

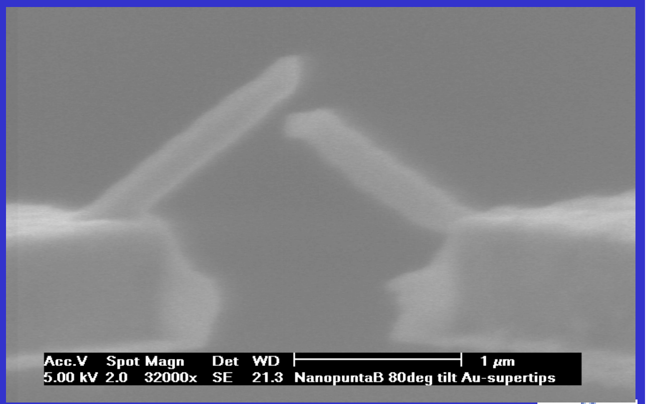

Focused Ion Beam - microsculpture

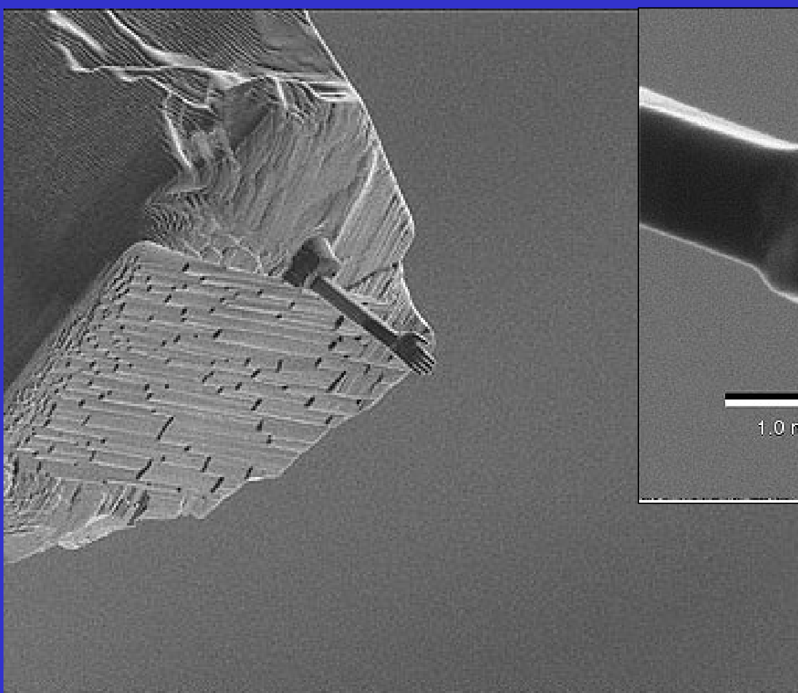

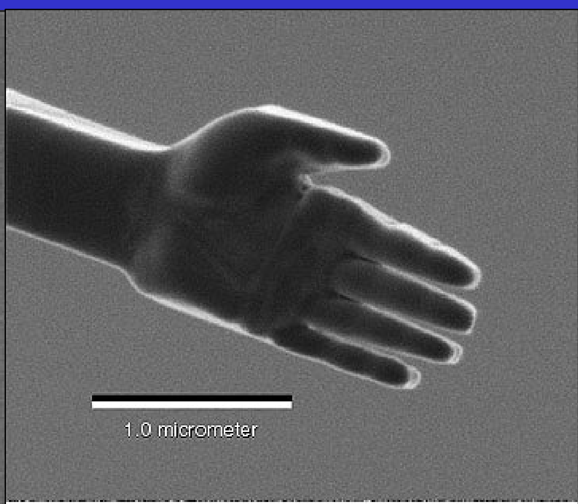

Microsculpture by FIB

Courtesy by LEO

3D manipulation et al:Optical Tweezers, Two Photon lithography, two photon microscopy

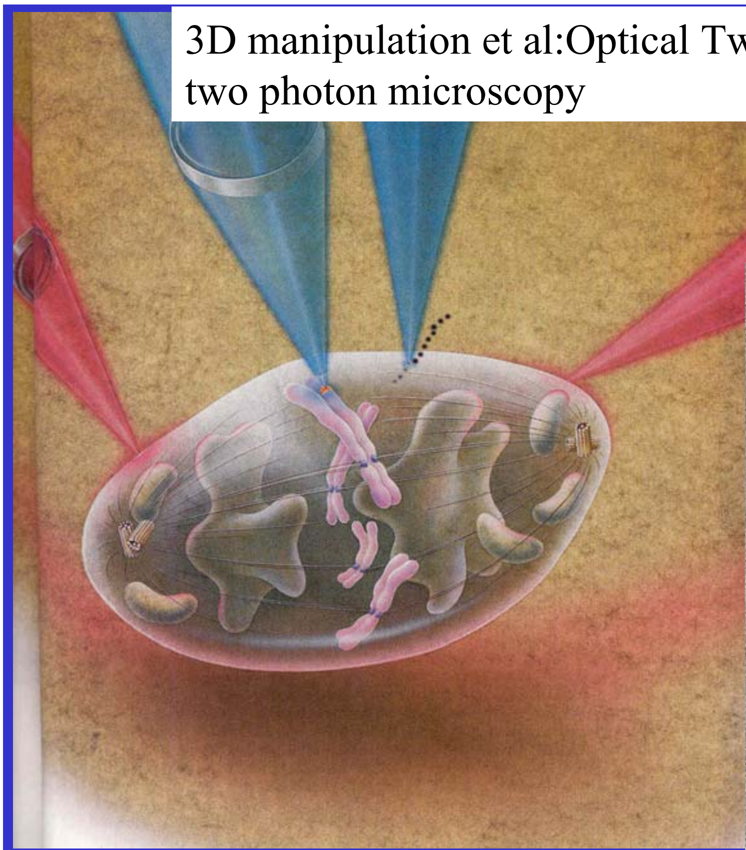

L'uso combinato di forbici e pinze laser consente di effettuare delicate manipolazioni a livello subcellulare. Nella procedura illustrata, che dovrebbe essere realizzabile entro una decina d'anni, due fasci che fungono da pinze (*in rosa*) trattengono strettamente la cellula. Un fascio forbice (*in blu chiaro*) penetra nella cellula per eliminare un gene difettoso (*in rosso*). Un secondo fascio forbice (*in blu scuro*) crea nella membrana cellulare un foro attraverso il quale potrà entrare una sequenza genica appropriata (*punti neri*). Si potranno poi ottenere cloni della cellula modificata che saranno trapiantati a scopo terapeutico.

Optical tweezers - background

INFM-ELETT

How do Optical Tweezers work ?

Two regimes of operation:

- Rayleigh regime (size of particle << λ)
- Mie regime (size of particle > λ)

Ashkin, A.; Dziedzic, J. M.; Bjorkholm, J. E.; and Chu, S., "Observation of a Single-Beam Gradient Force Optical Trap for Dielectrical Particles", Optics Letters 11, pp 288-290 (1986) - ray optics model

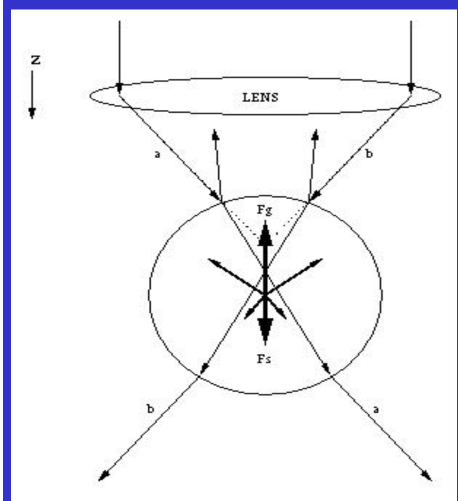

Two main forces:

- Scattering force, $\mathbf{F_s}$
- Gradient force, $\mathbf{F_g}$

$\mathbf{F = F_g + F_s}$

Rayleigh regime

$$F_s = \frac{8}{3}\pi\left(k^4 d^4\right)d^2 \frac{\sqrt{\varepsilon_0}}{c}\left(\frac{\varepsilon-\varepsilon_0}{\varepsilon+2\varepsilon_0}\right)^2 S$$

$$\mathbf{F_g} = 2\pi\mathbf{d}^3 \frac{\sqrt{\varepsilon_0}}{\mathbf{c}}\left(\frac{\varepsilon-\varepsilon_0}{\varepsilon+2\varepsilon_0}\right)\nabla|\mathbf{S}|$$

S - Poynting vector
d - size of particle
ε - dielectric constant of particle
ε_0 - dielectric constant of medium
k- wavenumber

Implementation of multiple optical tweezers using diffractive optical elements

2D arrays

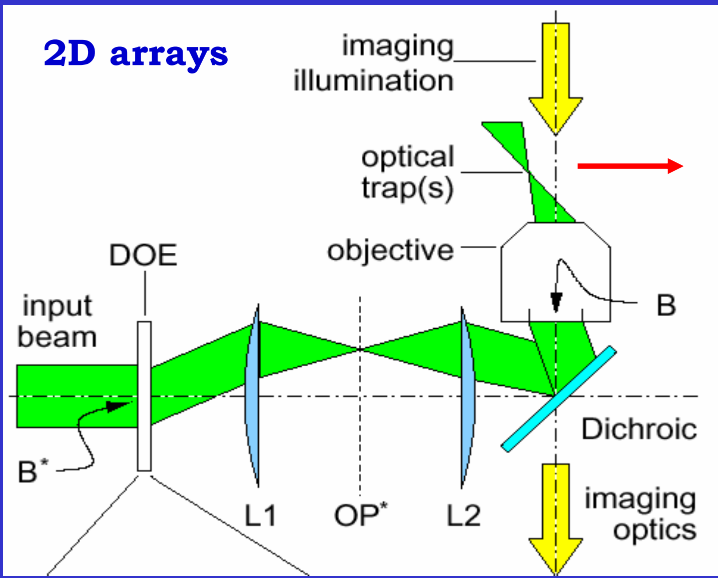

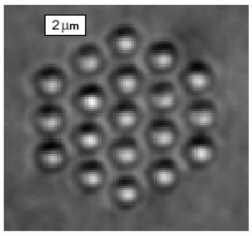

LILIT

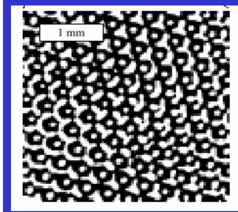

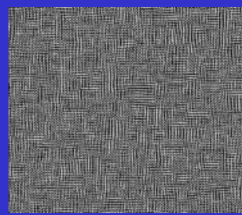

Eric R. Dufresne, Gabriel C. Spalding, Matthew T. Dearing, Steven A. Sheets, and David G. Grier, 'Computer Generated Holographic Optical Tweezer Arrays', *Rev. Sci. Instr.* **72**, 1810-1816 (2001).

Implementation of multiple optical tweezers using diffractive optical elements

3D arrays

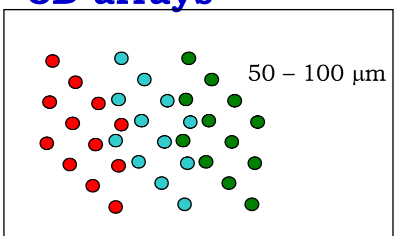

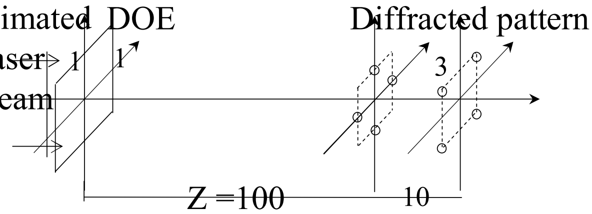

Fabricated DOE, detail~ 500 μm

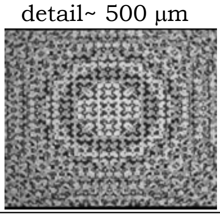

Intensity distributions:

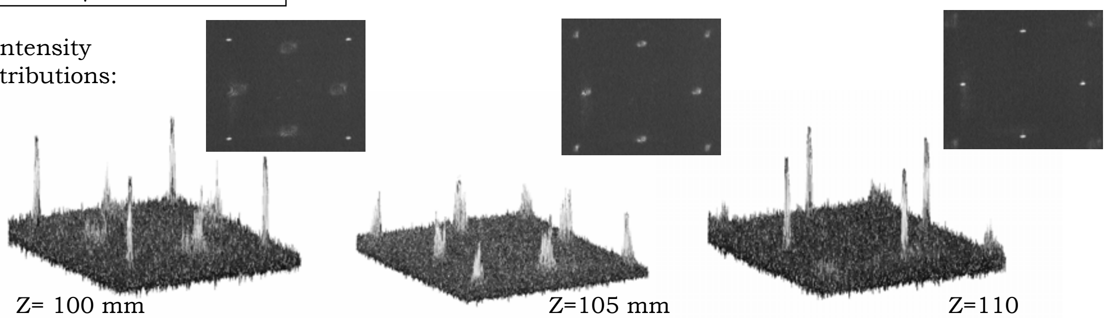

D. Cojoc, E Di Fabrizio, L. Businaro, S.Cabrini, F. Romanato, L. Vaccari, M. Altissimo, "Design and fabrication of diffractive optical elements for optical tweezer arrays by means of e-beam lithography", Microelectronic Engineering, 61-62, 963-969, 2002

Implementation of multiple optical tweezers using diffractive optical elements

Spherical wave approach

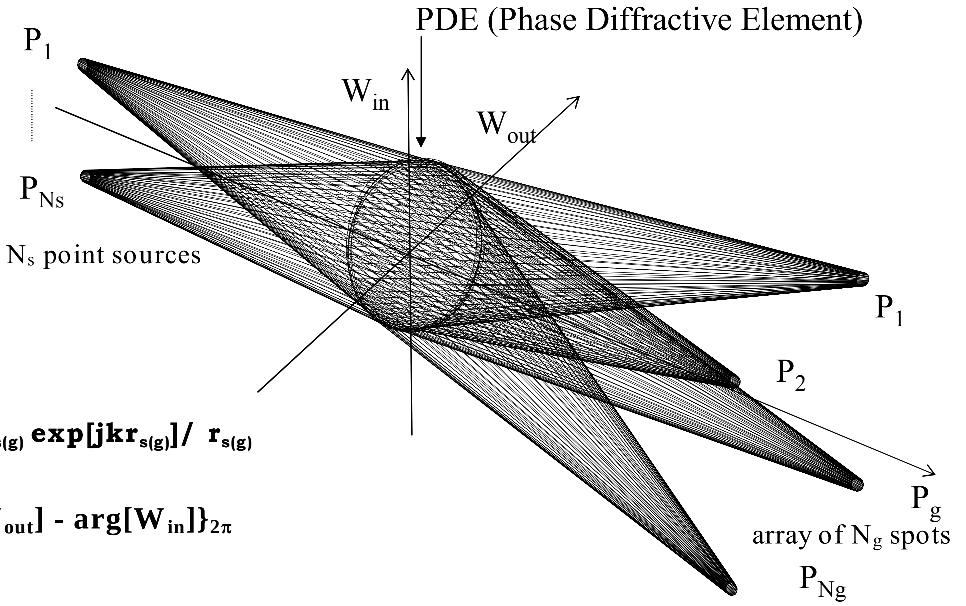

$$W_{in(out)} = \sum_{s(g)} a_{s(g)} \exp[jkr_{s(g)}] / r_{s(g)}$$

$$\Phi_{PDE} = \{\arg[W_{out}] - \arg[W_{in}]\}_{2\pi}$$

To estimate the phase function Φ_{PDE}, we assume that the light source which illuminates the PDE and the intensity distribution produced by the PDE can be described by point sources generating spherical waves

Dynamic optical tweezers – setup at LILIT

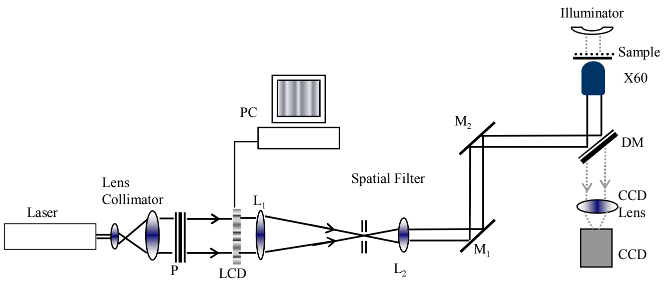

Optical Setup

P – polarizer

L1, L2 - convergent lenses

M1, M2 mirrors

DM – dichroic mirror

LCD Spatial Light Modulator

LC2002 Holoeye

Pixels	Pixel Pitch	Fill Factor	Panel Size	Addressing	Signal Formats
832 x 624	32 µm	85 %	21 x 26 mm	8 bit (256 values)	VGA, SVGA, Mac, PC98

Inverted microscope Nikon TE2000-E

Experimental results

2 D – Array of optical tweezers

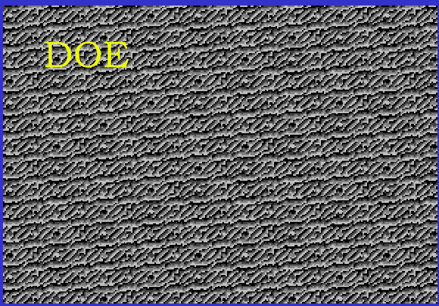

Microspheres of silica (diameter: 2 μm) immersed in water

The microscope stage is moved during the movie to show the stability of the traps

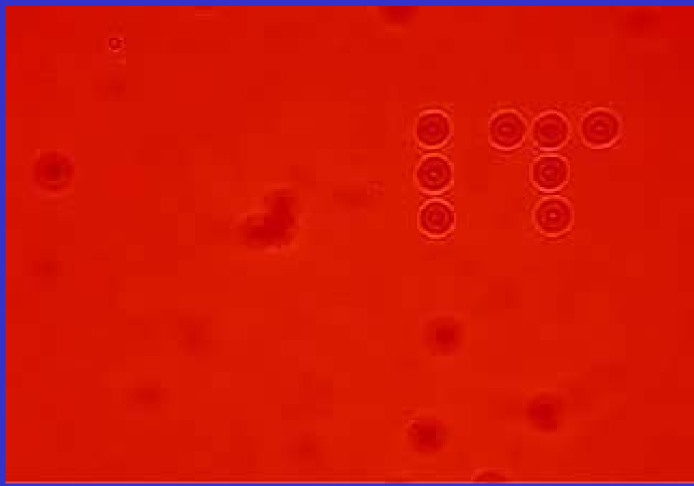

10 microns

Experimental results

Independent movement of trapped particles (2)

2 microspheres are trapped:
1 – on a circle (diameter 18 μm), rotating clockwise
1 – on a circle (diameter 13 μm), rotating anti-clockwise

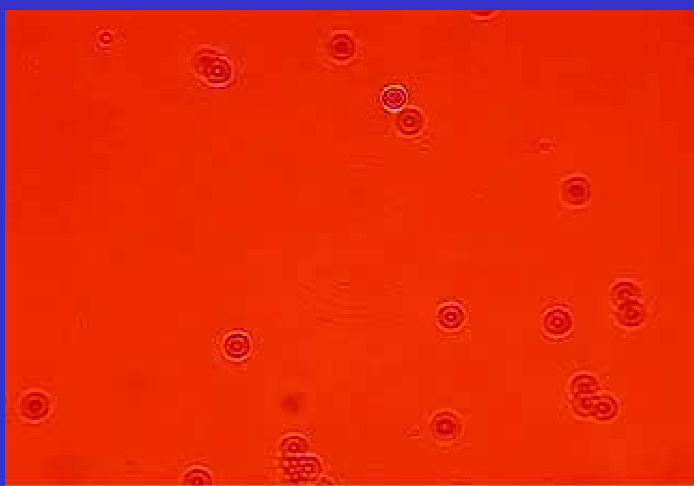

10 microns

Experimental results

3D displacement (2)

3 microspheres are trapped and moved in X-Y-Z

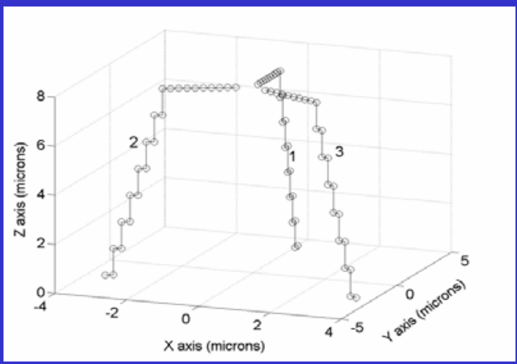

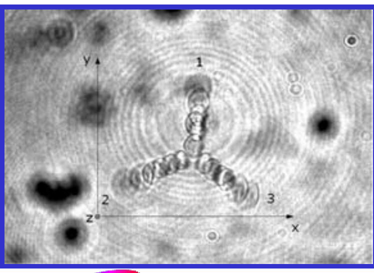

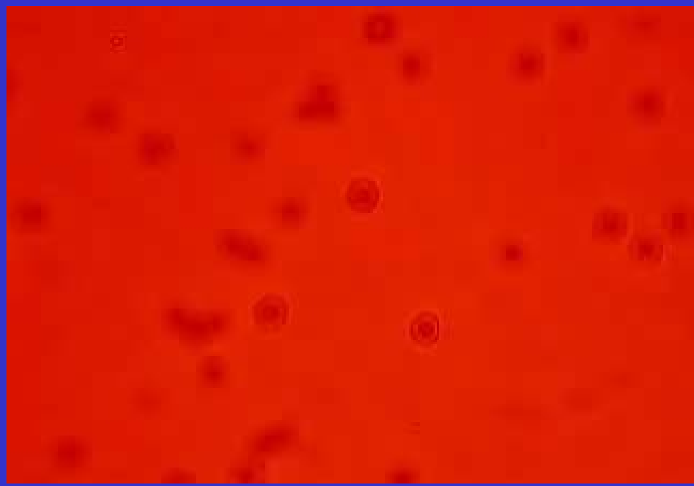

10 microns

Experimental results

Generating doughnut beams

Helical mode beam: $E(r,\theta,z) = E_0 \exp(il\theta)\exp(-ikz)$

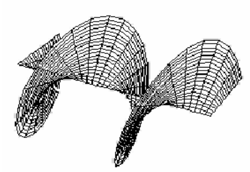

Uniform plane wave: $u = \exp(-ik_x x - ik_z z)$

Interference pattern: $I = 1 + E_0^{\,2} + 2E_0 \cos(k_x x - l\theta)$

The radius of the doughnut: $R_\ell = a \frac{\lambda f}{\pi \Sigma}\left(1 + \frac{\ell}{\ell_0}\right)$ f – focal length; a, Σ, l_0 - constants

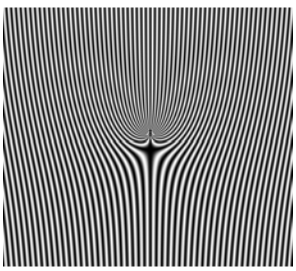

DOE

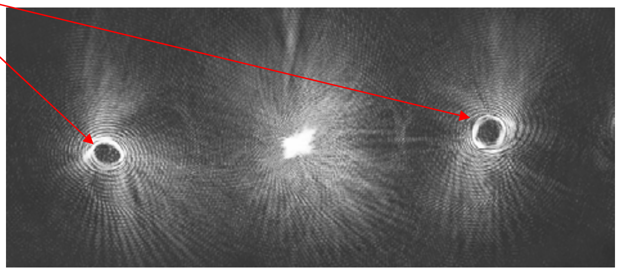

Intensity of the diffracted pattern

J.E. Curtis, D.G. Grier, 'Structure of optical vortices', PRL **90**, April 2003

Experimental results

Transfer of orbital angular momentum with doughnut beams

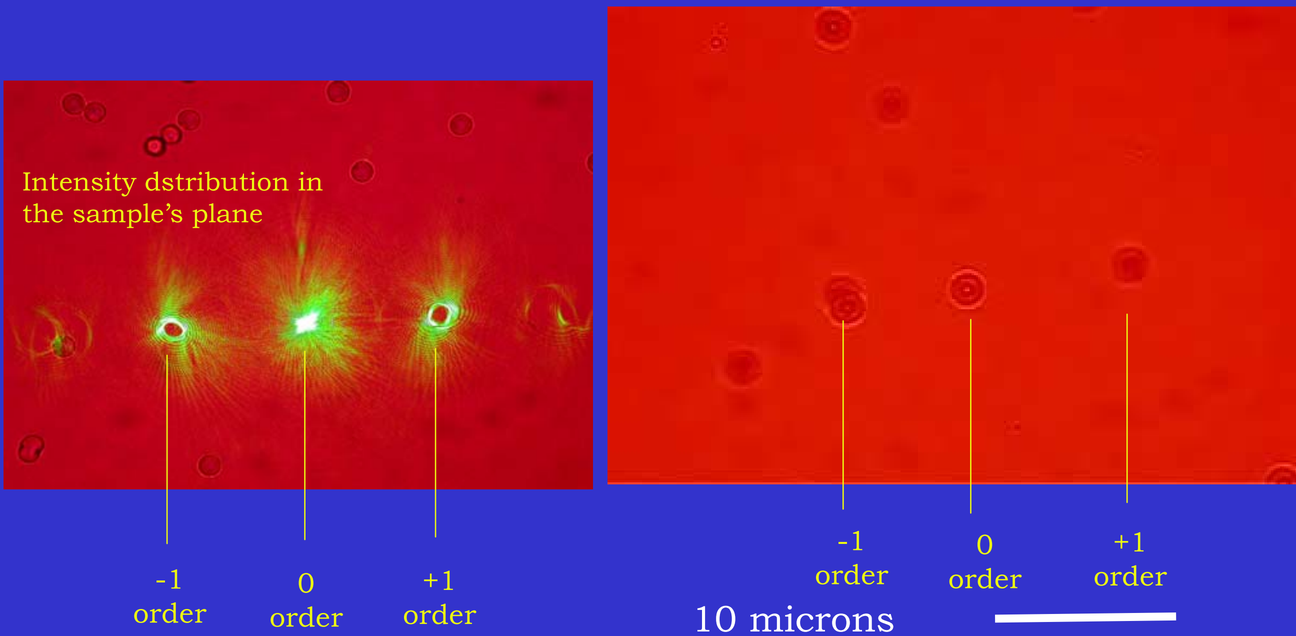

External Force Gradients and Cell Polarity (Collaboration with V. Emiliani- Jacques Monod Institute)

Cell Polarity: Cells organize functionally distinct sub-cellular domains to get into different processes.....

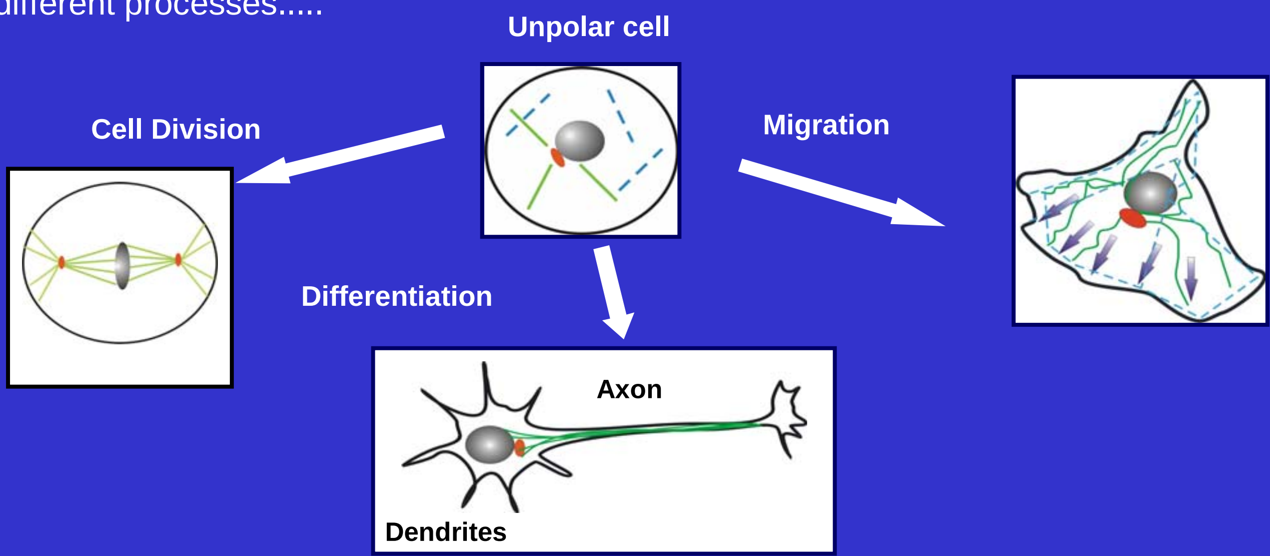

Polarity is usually initiated in response to extracellular cues (chemical or mechanical)

...a key role is played by the cell capability to sense mechanical gradients and tensions in the environment

- Durotaxis: cell movement can be guided by physical interactions at the cell-substrate interface

  Lo CM, Wang HB, Dembo M, Wang YL, Biophys. J 79, 144 (2000)

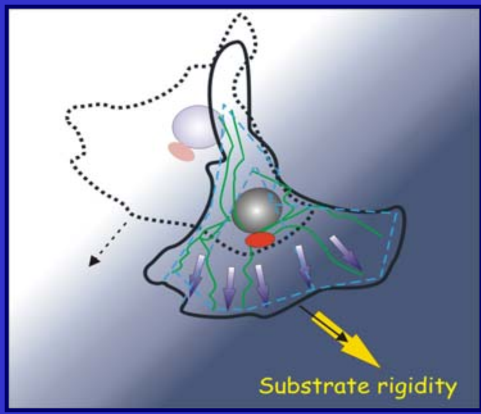

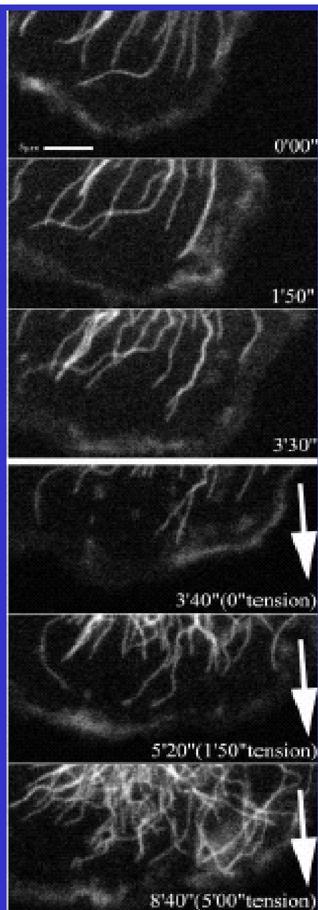

- Tensile stress: stimulate Microtubule outgrowth, RAC (GTPAses) activity, axons growth

  via micro-needles and flexible substrates

I. Kaverina et al. J. Cell Science 115, 2283 (2002)
S. Chada et al. J. Cell Science 110, 1179 (1997)

  equi-biaxial stretch device

Akira Katsuni et al. J Cell Biol. 158, 153 (2002)

Adherent cells will be plated on suitable arrays of ECM ligands coated beads

ECM ligands coated beads
2-6 μm

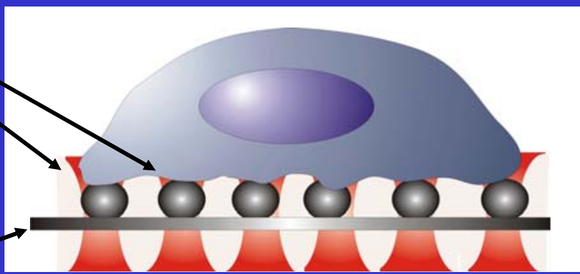

Non adherent substrate

Via the manipulation of the array we can induce controlled tension and/or mechanical gradients on the cell cortex in a low intensity range of forces

Force gradient

The trapping force is proportional to the laser intensity:
by making an array of laser spots with a gradient in intensity we can mimic a gradient in the substrate rigidity

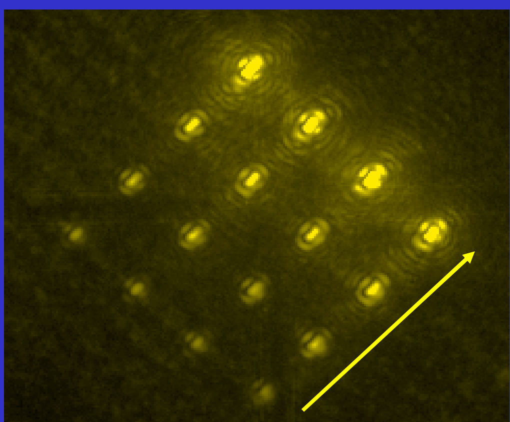

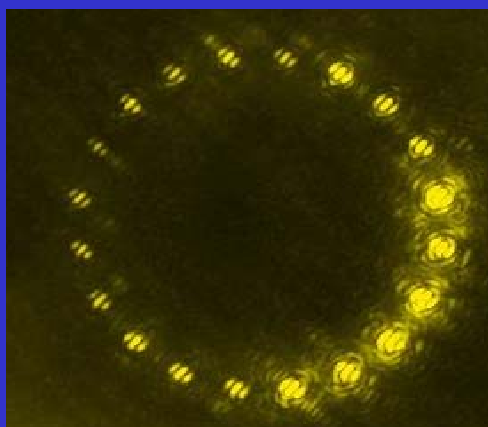

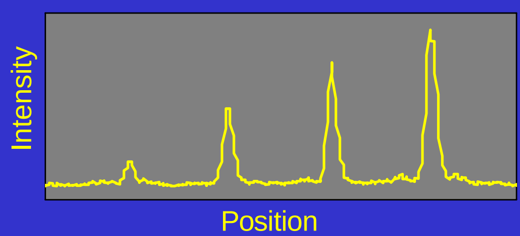

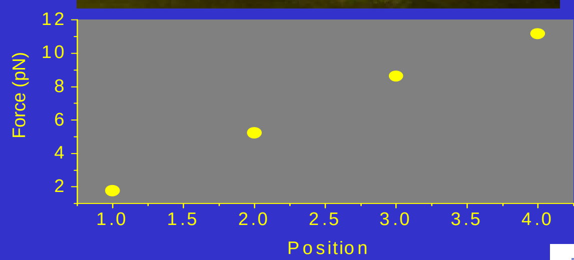

Mechanical stress

The all array can be deformed in a symmetric or asymmetric way:

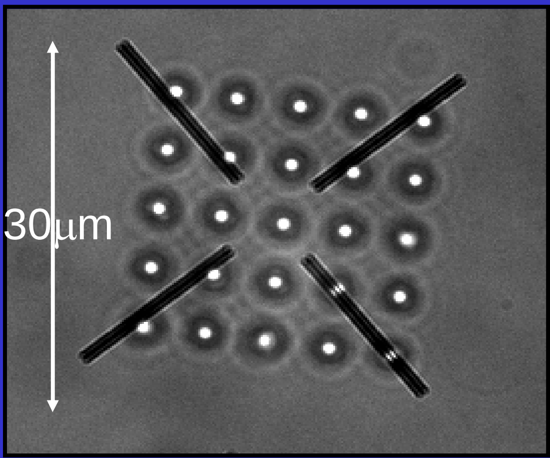

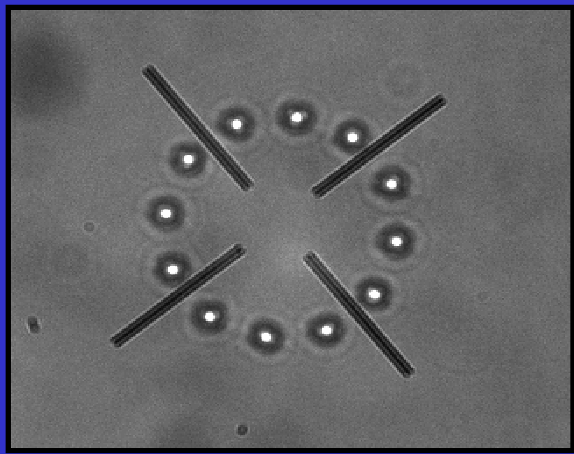

National Nanotechnology Laboratories
ICTP winter college 7-18 Febbraio 2005 Trieste
TASC - INFM

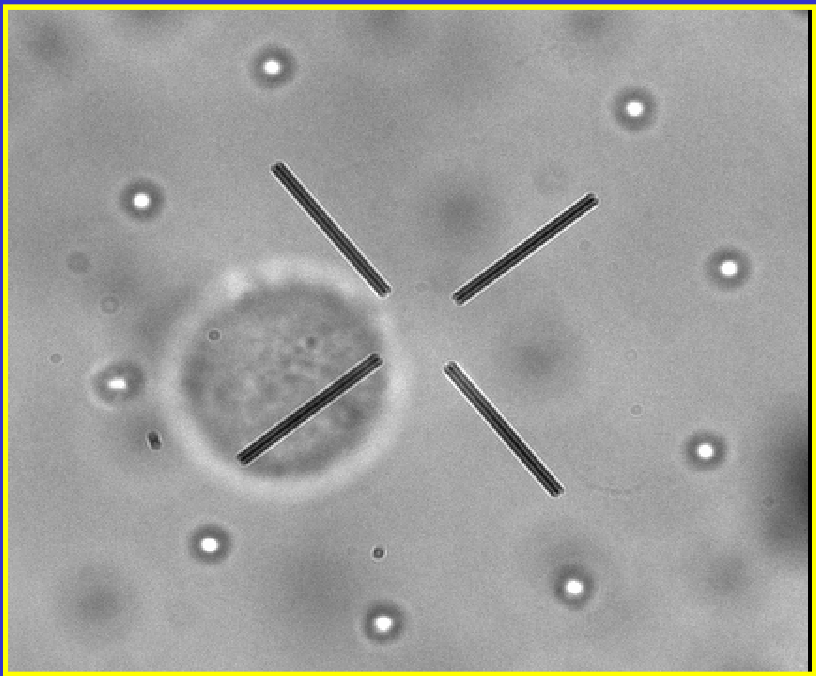

Imaging: Microtubules and Actin network organization

Cells close to *in vivo* conditions → reduced cell spreading

good axial resolution
+
fast acquisition time
→ Multi foci two photons Microscope
TriMScope, La Vision Biotec Gmbh, Germany

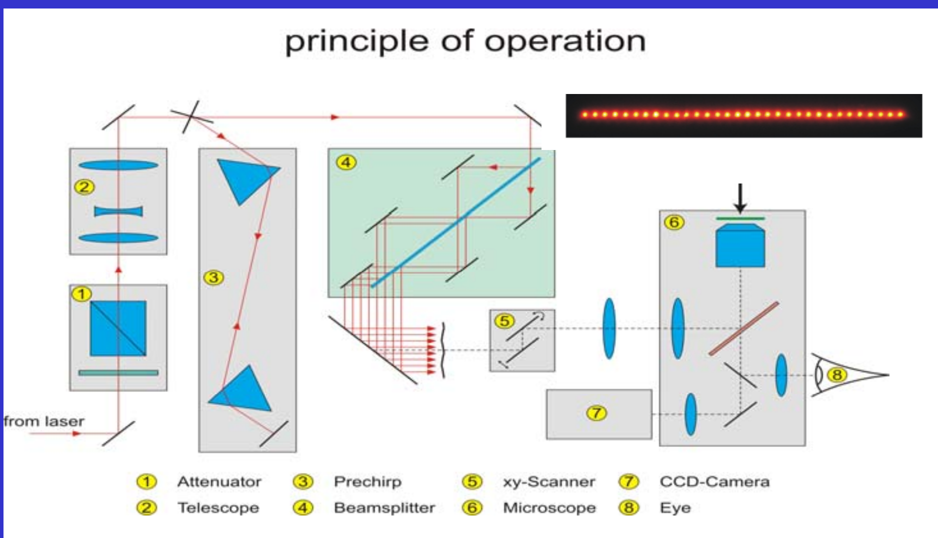

National Nanotechnology Laboratories
ICTP winter college 7-18 Febbraio 2005 Trieste
TASC - INFM

Imaging: Microtubules and Actin network organization

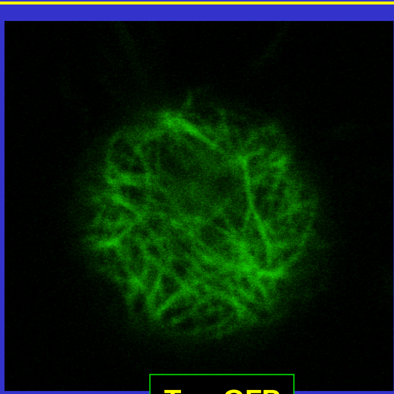

bottom

Tau GFP

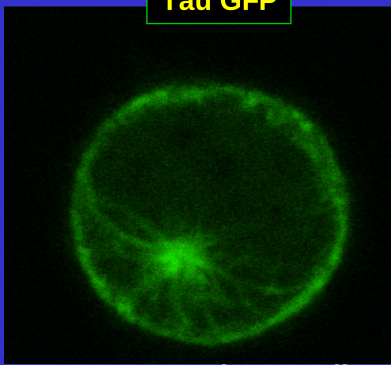

intermediate

ND7 Neuronal type cell

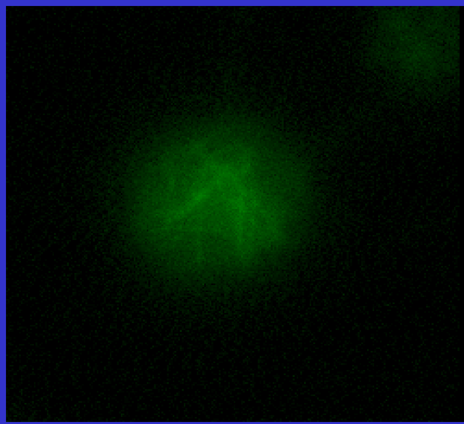

Optical manipulation of liposomes as microreactors

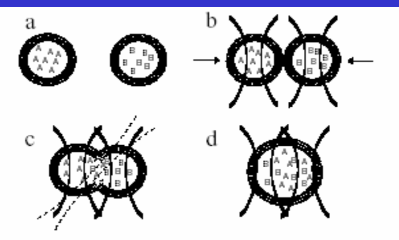

Figure 2: Schematic representation of the procedure for the trapping and fusion of two liposomes, containing different chemicals. a) Two liposomes, one containing reagent A and the other one containing reagent B, are identified in the sample. b) The two liposomes are trapped in separate optical tweezers and translated such that their membranes come into contact. c) Fusion is initiated by a pulsed UV laser, which disrupts the membranes of both liposomes at the contact point. d) The membranes repair spontaneously by forming one larger liposome in which the reagents A and B mix.

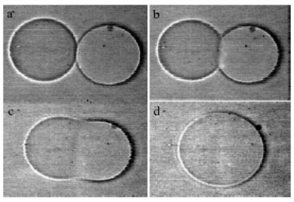

Figure 3: Fusion of two liposomes. The images are recorded by video microscopy. The fusion was initiated by the UV laser at the time when the first image was recorded. The next two images capture the progression of the fusion process at 132 ms and 264 ms, respectively. The last image, recorded at 528 ms, shows one single large liposome formed as a result of the fusion.

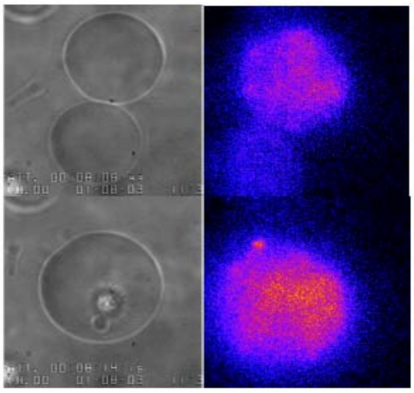

Figure 6: Fusion of two liposomes, one containing fluo-3 dye and the other one containing calcium ions. The bright field video microscopy images and the fluorescence images recorded simultaneously before and after the fusion was initiated (upper and lower images, respectively). After the fusion the fluorescence increases as a consequence of the reaction in which fluo-3 chelates the calcium ions.

Simone Kulin*, Rani Kishore*, Kristian Helmerson*, Laurie Locascio†
*Physics Laboratory and †Chemical Science and Technology Laboratory,
National Institute of Standards and Technology, Gaithersburg, MD 20899

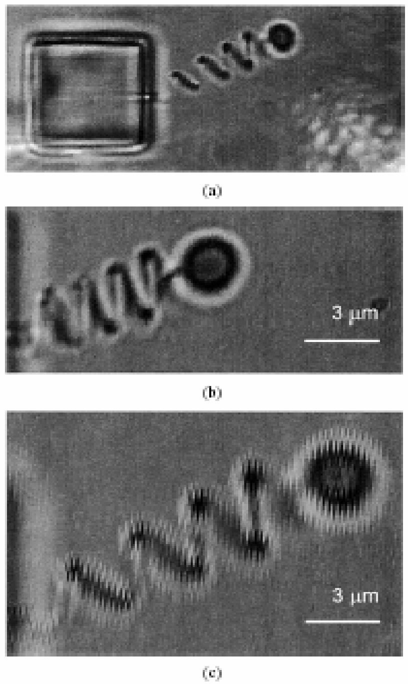

Fig. 10. A functional microoscillator system. (a) Photomicroscopic image of the microoscillator, which consists of an anchor fixed to the glass substrate, a microspring with core diameter of 300 nm, and a spring-end-attached microsphere. (b) The spring was pulled to a length and kept there. (c) Spring restored to its original length.

Two photon and optical tweezers

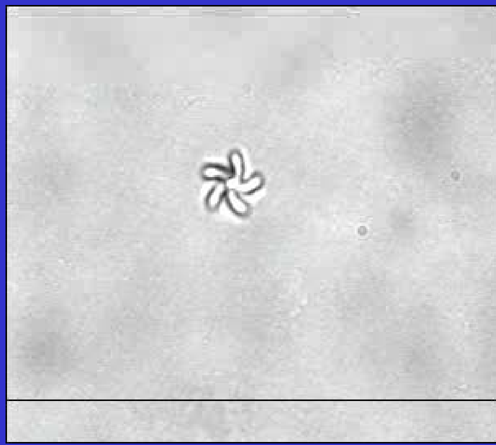

National Nanotechnology Laboratories

ICTP winter college 7-18 Febbraio 2005 Trieste

TASC - INFM

OT & TPE:Solid and Hollow nanocapsules

Confocal Laser Scanning Microscopy (**CLSM**) of capsules (green) with ionic core (black) inside and Rhodamine (red) outside

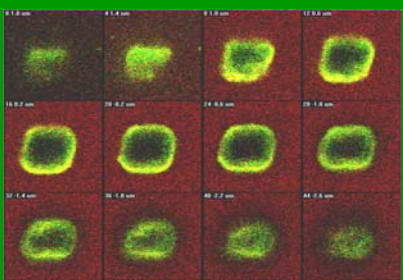

Atomic force microscopy (**AFM**) of dried empty capsules

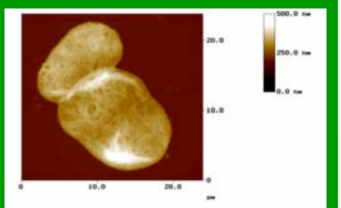

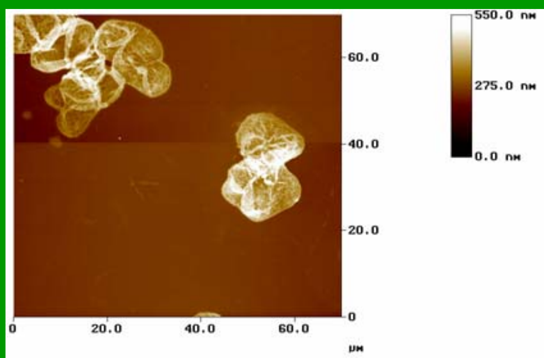

Two-Photon Excitation Fluorescence microscopy (**TPE-FM**) and optical microscopy of encapsulated (green) and duplicated yeast

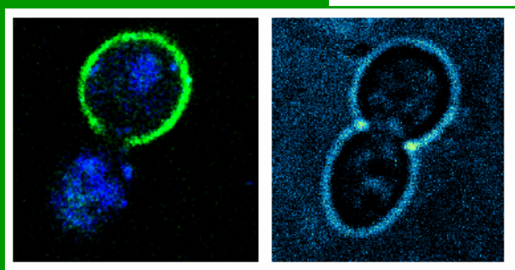

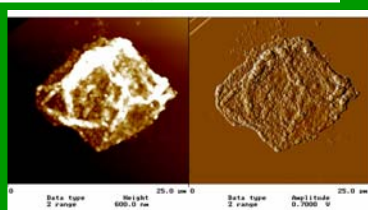

QuickTime™ and a
GIF decompressor
are needed to see this picture.

UdR 4 - Genova

National Nanotechnology Laboratories

ICTP winter college 7-18 Febbraio 2005 Trieste

TASC - INFM

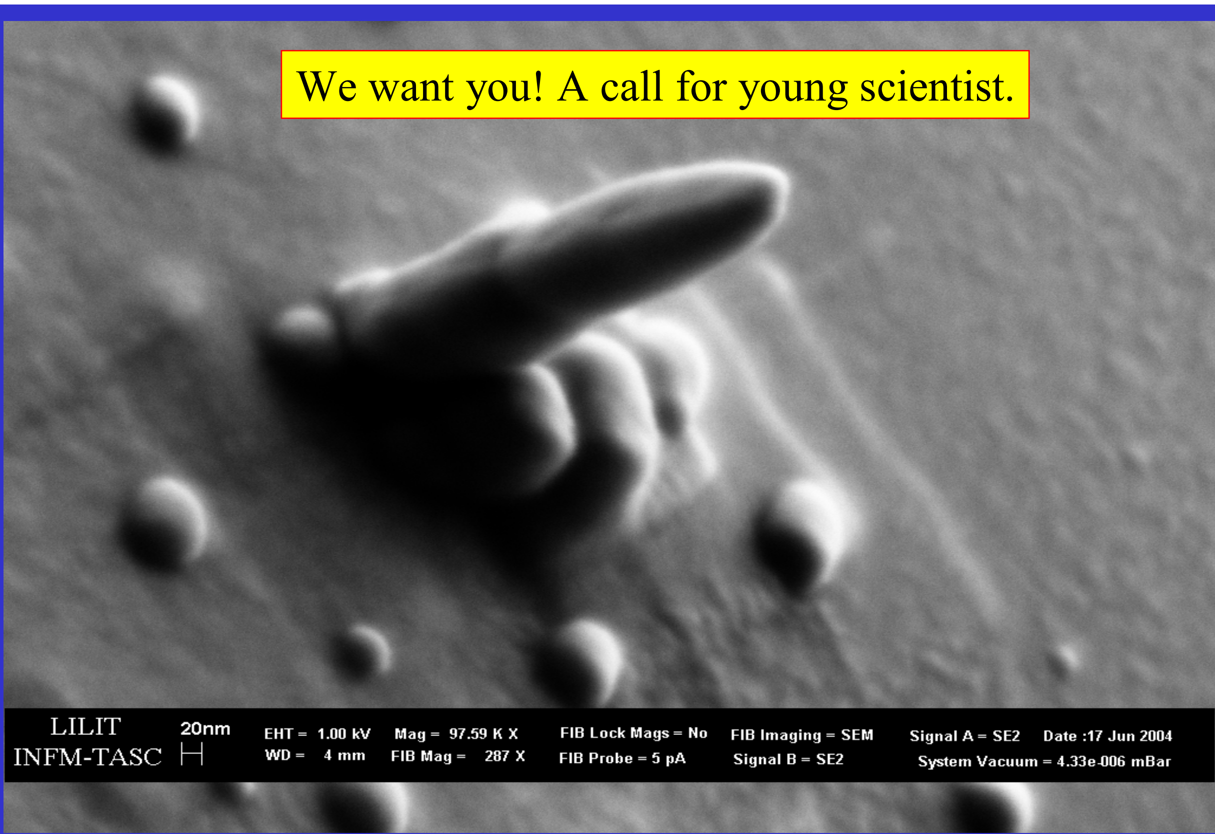

Acknowledgements

Micro & naofabrication team

E. Di Fabrizio, F. Romanato, S. Cabrini, F. Perennes,

D. Cojoc,L. Vaccari, V. Garbin, E. Ferrari, M. Altissimo, L. Businaro, P. Candeloro,, M. Tormen, M. Radu, A. Gosparini, Revati

A. Carpentiero, M. Prasciolu, M. Matteucci,R. Kumar

G. Quondam

National Nanotechnology Laboratories
ICTP winter college 7-18 Febbraio 2005 Trieste
TASC - INFM